# Strengthening of the Air Quality Information System

# Working area 2: Application of a regional-scale model over the central part of Chile

-

## REGIONAL DISPERSION OF OXIDIZED SULFUR OVER CENTRAL CHILE: A FALL CASE

**G. Olivares and L. Gallardo**
*National Commission for the Environment, Chile*
*and*
**J. Langner and B. Aarhus**
*Swedish Meteorological and Hydrological Institute, Sweden*

**June 2000**

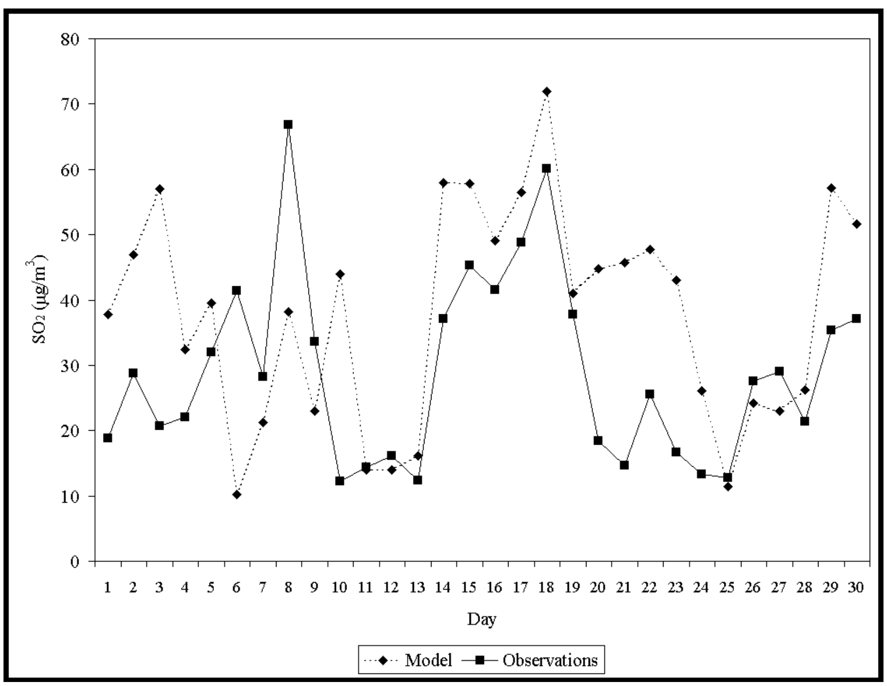


*Daily averages for Santiago as calculated by HIRLAM-MATCH and as observed in May 1998*

**TABLE OF CONTENTS**

# DISPERSIÓN REGIONAL DE AZUFRE OXIDADO EN CHILE CENTRAL: UN CASO DE OTOÑO

**G. Olivares y L. Gallardo**

*Comisión Nacional del Medio Ambiente, Chile*

*y*

**J. Langner y B. Aarhus**

*Instituto Sueco de Meteorología e Hidrología, Suecia*

## RESUMEN

La dispersión regional de compuestos oxidados de azufre en Chile central en Mayo de 1998 es simulada con un modelo Euleriano de área limitada (MATCH). Los patrones meteorológicos son simulados a través de un modelo meteorológico de área limitada (HIRLAM). Mayo de 1998 es un período interesante pues entonces tuvo lugar un evento extremo de contaminación. Las simulaciones han sido comparadas con las observaciones de modo de evaluar el modelo para condiciones otoñales. Este ejercicio debe considerarse complementario al caso estival antes presentado. Adicionalmente, se ha hecho un análisis de los datos de dióxido de azufre ($SO_2$) reportados por varias redes de monitoreo para Mayo de 1998.

Las observaciones muestran claros ciclos diarios en $SO_2$ en la mayoría de las estaciones de monitoreo. Estos ciclos están típicamente asociados a la presencia de circulaciones radiativas y a variaciones en las emisiones locales, principalmente aquellas asociadas a fuentes móviles o de transporte. Además, las concentraciones varían fuertemente día a día. Esta variación se asocia a los cambios en las condiciones sinópticas que afectaron a Chile central en Mayo de 1998. El patrón más notable corresponde a un severo episodio de contaminación (Mayo 15 a 20). Este episodio estuvo asociado a una intensa baja costera, es decir, una situación en la cual prevalece una inversión de subsidencia intensificada que suprime la mezcla vertical.

El modelo meteorológico reproduce las principales características de la circulación durante Mayo de 1998. En particular, simula bien las condiciones meteorológicas asociadas a una baja costera en Chile central que se propaga por la costa al sur (Configuración tipo A). Las condiciones prefrontales que preceden a un frente débil u ocluido que se tiende a detener o a hacerse estacionario (Configuración BPF) no son tan bien simuladas. Al menos durante la primera mitad de Mayo 1998. Las discrepancias se asocian a una subestimación de la cobertura nubosa que induce una sobreestimación de las circulaciones radiativas.

Como en el caso veraniego, las emisiones de las fundiciones de cobre dominan la distribución horizontal y vertical del azufre en Chile central. La contribución de las fuentes urbanas en zonas rurales así como por sobre la capa límite se estima en menos de 10%. Además, las fundiciones de cobre contribuyen episódicamente al contenido de azufre dentro de las zonas urbanas. Dicho impacto parece relacionarse con la fuerte y generalizada subsidencia asociada con la configuración tipo A de Mayo de 1998. Los cálculos del modelo indican una conexión entre el impacto episódico y la aparición de masas de aire envejecidas, con tasas de sulfato sobre $SO_2$ más altas, esto es, asociadas a aerosoles secundarios en Santiago. Salvo efectos locales, sobre una base de promedios diarios, el modelo generalmente reproduce las observaciones. Especialmente, MATCH reproduce el episodio tipo A. Sin embargo, el modelo no incluye el sumidero asociado a las condiciones de neblina que ocurren al final del episodio. Los ciclos diarios también son generalmente bien reproducidos por el modelo. No obstante, existen discrepancias sustantivas. Algunas en conexión con falencias de la base de datos de emisiones. Otras en conexión con limitaciones en la representación de los campos meteorológicos.

La validación del modelo continuará. Además de los casos de verano y otoño ya presentados, serán evaluadas situaciones de primavera y verano y dos situaciones de invierno. También, en un informe venidero, se abordará en más detalle el tema de la partición entre los reservorios de azufre de $SO_2$ y sulfato.

# REGIONAL DISPERSION OF OXIDIZED SULFUR OVER CENTRAL CHILE: A FALL CASE

**G. Olivares and L. Gallardo**

*National Commission for the Environment, Chile*

*and*

**J. Langner and B. Aarhus**

*Swedish Meteorological and Hydrological Institute, Sweden*

## ABSTRACT

The regional dispersion of oxidized sulfur in Central Chile for May 1998 is simulated with a limited area, Eulerian transport model (MATCH). The meteorological features are simulated through a meteorological limited area model (HIRLAM). May 1998 is an interesting period since an extreme pollution episode took place at that time. The simulations have been compared with the observations in order to assess the model performance under fall conditions. This exercise must be considered complementary to the summer case presented in an earlier report. Additionally, an analysis of the sulfur dioxide ($SO_2$) data provided by several networks for May 1998 has been made.

The observations show distinct diurnal cycles in $SO_2$ at the majority of the monitoring stations. These cycles are typically associated with the presence of radiative circulations and variation in local emissions, mainly in connection with transportation sources. In addition, a strong day-to-day variation in the concentrations is apparent. This variation is linked to the variations in the synoptical patterns that affected Central Chile in May 1998. The most outstanding feature was a rather sever air pollution episode (May 15$^{th}$ through May 20$^{th}$). This episode was associated with a strong low-level low, i.e., a situation for which a depressed subsidence inversion prevails ahead of the low and leads to suppressed vertical mixing.

The meteorological model is able to simulate the main features of the circulation for May 1998. In particular, it reproduces well the meteorological conditions associated with the onset of a coastal low in Central Chile moving southward along the coast (A type configuration). The prefrontal conditions ahead of a weak and often occluded front that slows down or becomes stationary (BPF type configuration) is less well captured. At least during the first half of May 1998. The disagreements are linked to underestimates of cloud cover, which in turn result in too strong thermally driven circulations.

As for the summer case, the emissions from the copper smelters dominate the overall horizontal and the vertical distribution of sulfur in Central Chile. The contribution of urban sources at rural sites as well as above the boundary layer is estimated to be less than a 10%. Moreover, the copper smelters contribute episodically to the oxidized sulfur burden inside the urban areas. That impact appears to be related to the strong general subsidence associated with the A type configuration in May 1998. The model calculations show a connection between the episodic impact of the copper smelters and the appearance in Santiago of aged air masses with higher sulfate to $SO_2$ ratios, i.e., associated with secondary aerosols. Except for local effects, on a daily average basis, the model generally reproduces the observations. In particular, MATCH reproduces the A-type episode. However, it does not include a sink process in connection with foggy conditions that take place at the end of the episode. Also the diurnal cycles are generally well simulated by the model. Significant discrepancies occur though. Some are in connection with inaccuracies in the emission database. Some other are related to shortcomings in the representation of the meteorological fields.

The validation of the modeling tool will continue. In addition to the summer and fall scenarios already presented, a spring and summer situation, and two winter situations will be evaluated. Also, in an up-coming report we will address the issue of the partitioning between the $SO_2$ and sulfate reservoirs in more detail.

# 1. INTRODUCTION

In 1999, a cooperation project between the National Commission for the Environment (CONAMA) and the Swedish Meteorological and Hydrological Institute (SMHI) was initiated (See http://www.swe-chile.com for details). Through this project, we attempt to assess the regional distribution of man-made pollutants, mainly oxidized sulfur, in Central Chile. Urban and regional air pollution problems of this type involve spatial and time scales that range from tens to hundreds of kilometers in the horizontal, a few kilometers in the vertical and from a few hours to several days in time (e.g., Seinfeld and Pandis, 1998). Therefore, local, meso-scale and synoptic transport patterns must be considered when assessing such problems. Through this joint CONAMA-SMHI effort, the dispersion of oxidized sulfur in Central Chile is simulated with a limited area, off-line, Eulerian transport model (MATCH). The meteorological features of Central Chile are simulated through a meteorological limited area model (HIRLAM). For details about the HIRLAM-MATCH system see Robertson et al. (1999).

Our work emphasizes the validation on a regional scale of the modeling tool (HIRLAM-MATCH) through a systematic comparison with available observations. In the case of the meteorological aspects, the validation has been performed by a systematic comparison of the simulations with data on wind speed and direction and temperature from a subset of the ca. twenty-two stations that have been installed in the Santiago basin. Available data from synoptic meteorological stations in the whole model area have also been utilized. In the case of dispersion, data provided by monitoring networks in Santiago and in the surroundings of industrial complexes have been utilized. It must be pointed out that the majority of the available monitoring stations have been placed to assess mainly local impacts, especially health effects. Therefore it cannot be expected that a regional model like HIRLAM-MATCH will be able to reproduce all the features of such observations. However, the systematic evaluation of the model simulations allows us to identify shortcomings in the emission inventories and to identify sites which should be considered in the design of a regional monitoring network. Furthermore, one must keep in mind that the validation of any model is a step-by-step, complex and in some respects never-ending process through which one can quantitatively and qualitatively assess the suitability of a model for a number of applications.

In the following pages, an evaluation of HIRLAM-MATCH for the fall scenario of May 1998 is presented. This is an interesting period since an extreme pollution episode took place at that time. This exercise must be understood as complementary to the one already presented (CONAMA-SMHI, 1999), which dealt with the evaluation of a summer scenario. Both steps, i.e., January and May 1998 scenarios, will be complemented by several tests, which will be performed for spring, and winter conditions in the up-coming reports.

In Section 2, the evaluation of the meteorological model (HIRLAM) is presented. In Section 3 the corresponding evaluation for the dispersion model (MATCH) is shown. The overall conclusions are summarized in Section 4.

# 2. METEOROLOGICAL SIMULATIONS (HIRLAM)

**J. Langner and B. Aarhus**
*Swedish Meteorological and Hydrological Institute, Sweden*

## 2.1. Introduction

In order to provide meteorological input data to the regional transport/chemistry/deposition model MATCH a three-dimensional numerical weather prediction model, HIRLAM, has been set up and executed for five month long periods over an area covering part of Chile. The result is a validated data set, which can be used for a range of studies using regional transport/chemistry/deposition models. Details of the set-up of HIRLAM were reported in the Advance report in December 1999 along with the evaluation of the first month simulated, January 1998. This document provides an evaluation of the first of four additional periods that have been simulated. For basic information about the HIRLAM model the reader is referred to the 1999 report (CONAMA-SMHI, 1999).

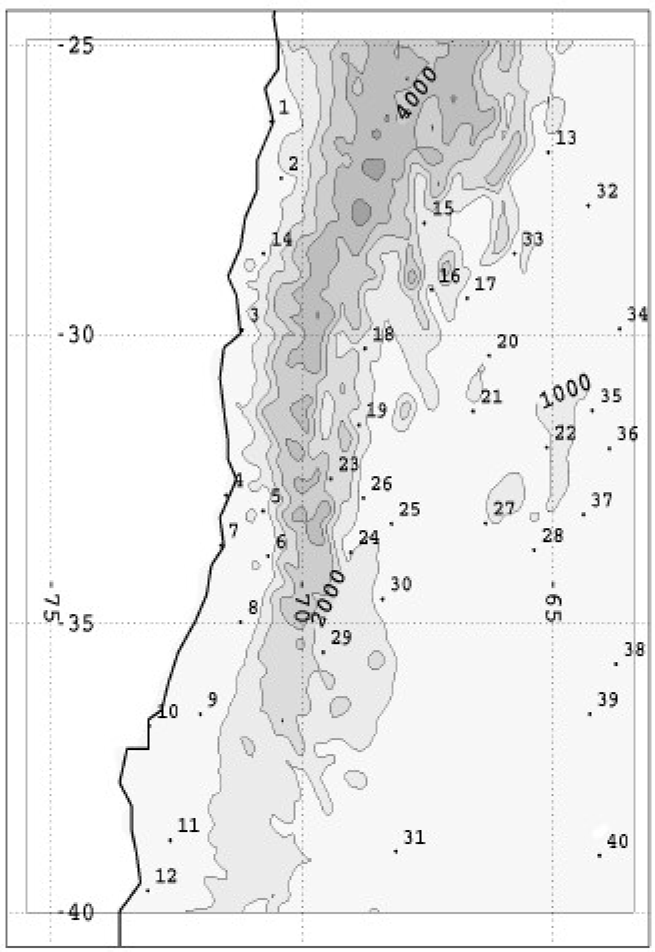


**Figure 2.1.** The model domain and meteorological stations from Table 2.1.

## 2.2. Set-up of HIRLAM

A HIRLAM-simulation for Chile, for a summer period, January 1998 has already been reported. Four additional periods have been simulated; a new summer situation, November-December 1999, and three fall/winter situations May-June 1997, May 1998 and June-July 1999.

Six hourly analyzed three-dimensional meteorological fields from the European Centre for Medium Range Weather Forecasts (ECMWF, http://www.ecmwf.int) operational model interpolated to 0.5°x0.5° (ca. 50x50 km) horizontal resolution was used as lateral boundary conditions for the HIRLAM simulations. For the periods in 1997 and 1998 the ECMWF-model had 31 levels, in June/July 1999 there were 50 layers and in November 1999 ECMWF started to use 60 layers. Sea surface temperature (SST) was also taken from ECMWF at six-hour intervals.

The results presented here were all derived with HIRLAM using a 0.1° (~11 km) horizontal resolution on a regular latitude longitude grid and 31 layers. The model domain for the simulation periods in 1997 and 1998 had 126x152 grid points horizontally but the simulations from 1999 are over a larger model domain, 126x250 grid points. The larger model area also includes the northernmost part of Chile. This was done in order to be able to use the meteorological information also for a parallel study of arsenic dispersion in Chile.

In January 1998 semi-lagrangian (SL) integration with a time step of 180 s was used. In the simulations described here, SL integration and 90 s time step has been used due to numerical stability problems with the convection processes in winter. Eulerian integration with a 60 s time step was also tested, but this did not have a significant effect on the results.

## 2.3. Evaluation strategy

Evaluation of the model simulations has focused on the central part of Chile and the area surrounding Santiago, which is the main area of interest in the project. In this area a meteorological network with 22 stations is operational. Data on wind speed and direction and temperature from four selected stations have been used from this network. The stations were chosen to cover different parts of the area and based on experience of station representativity and availability of data. The comparison was made in terms of time series plots and wind roses. Available data from synoptic meteorological stations reporting to the World Meteorological Organization (WMO) network in the whole model area has also been utilized. This includes surface data on wind speed and direction, temperature, humidity, precipitation, cloud cover and pressure at 40 stations as well as vertical profiles of wind speed and direction, temperature, humidity and geopotential at three locations. The locations of the synoptic meteorological stations are depicted in Figure 2.1, which also shows the model region that was used for the first three periods simulated. Figure 2.2 shows the meteorological network around Santiago. The synoptic meteorological stations are listed in Appendix I, Table A1 and the stations around Santiago in Table A2.

The data from the synoptic meteorological stations were used in a statistical evaluation of the model simulations. Up to eight observations per day were available for each of the synoptic stations. For the sounding stations two soundings per day were available. Root mean square error (RMS) and bias between the observations and HIRLAM simulations were calculated and averaged for the synoptic meteorological stations (See Appendix II for details). The same calculation was also made for the ECMWF analyses, which were utilized as boundary conditions for the HIRLAM simulations. Comparing the results for HIRLAM and ECMWF provides an overall measure of how well the HIRLAM simulation captures the synoptic conditions during the simulation period. The ECMWF analysis should be hard to beat since it is based on the observations but HIRLAM should be able to come close to ECMWF.

For selected synoptic stations also time series plots of observed and simulated data are examined to aid in the evaluation of the simulations. Maps of the model simulated cloud cover, wind and precipitation together with observations are shown for selected times during each simulation period to provide a picture of the observed and simulated synoptic conditions.

As the evaluation work has progressed the need for additional comparisons has become evident. In the final report we plan to include objective verification also for the stations in the Santiago regional network. The vertical structure of meteorological variables will also be discussed in more detail by examining time series of vertical profiles of turbulent kinetic energy, temperature, humidity and wind.

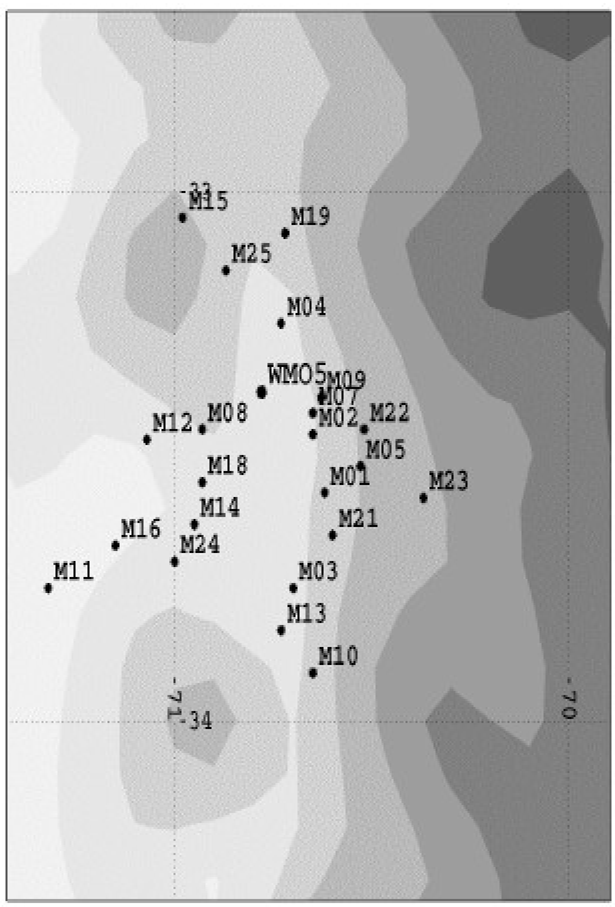


**Figure 2.2.** Map of the stations in the Santiago area, from Table 2.2. Pudahuel, (WMO-station number 5 in Table 2.1) is also marked. The topography is the one used in HIRLAM.

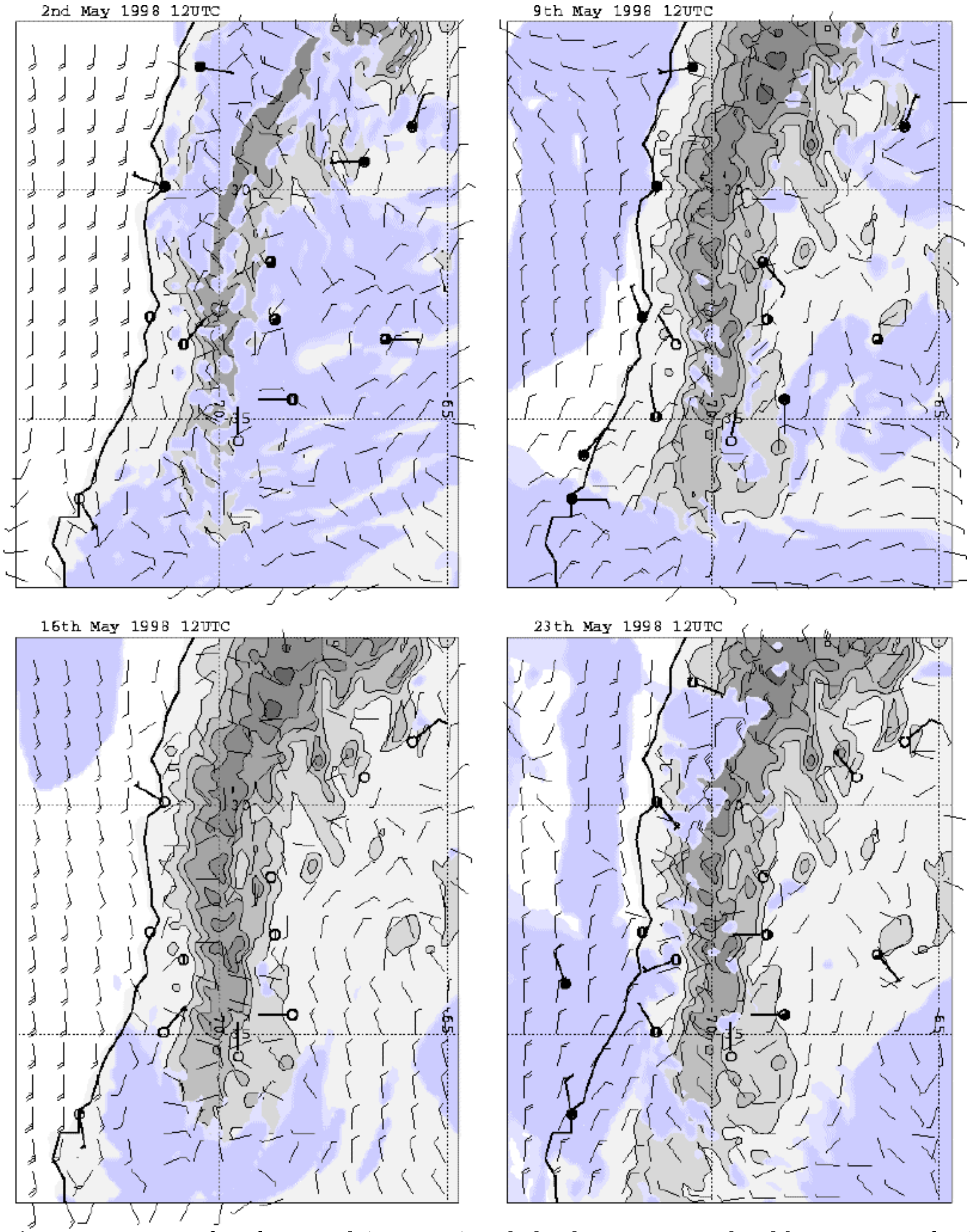


**Figure 2.3**. Maps of surface wind (10 meter) and cloud cover as simulated by HIRLAM for four different occasions during May 1998. Also shown is wind and cloud cover from available synoptic observations. The wind barb denotes wind speed and direction. The barb points in the direction the wind is blowing from. Speed is given in knots where half a barb represents 5 kts and a whole barb 10 kts. 2 kts is equal to 1 m/s. Note that the winds observed at the station close 35°S, 70°W seem to be in error. The filling of the station circle indicates observed cloud cover. A white circle corresponds to zero observed cloud cover while a filled circle indicates a completely cloud covered sky (eight octas). Partially filled station circles indicate partly cloud-covered conditions.

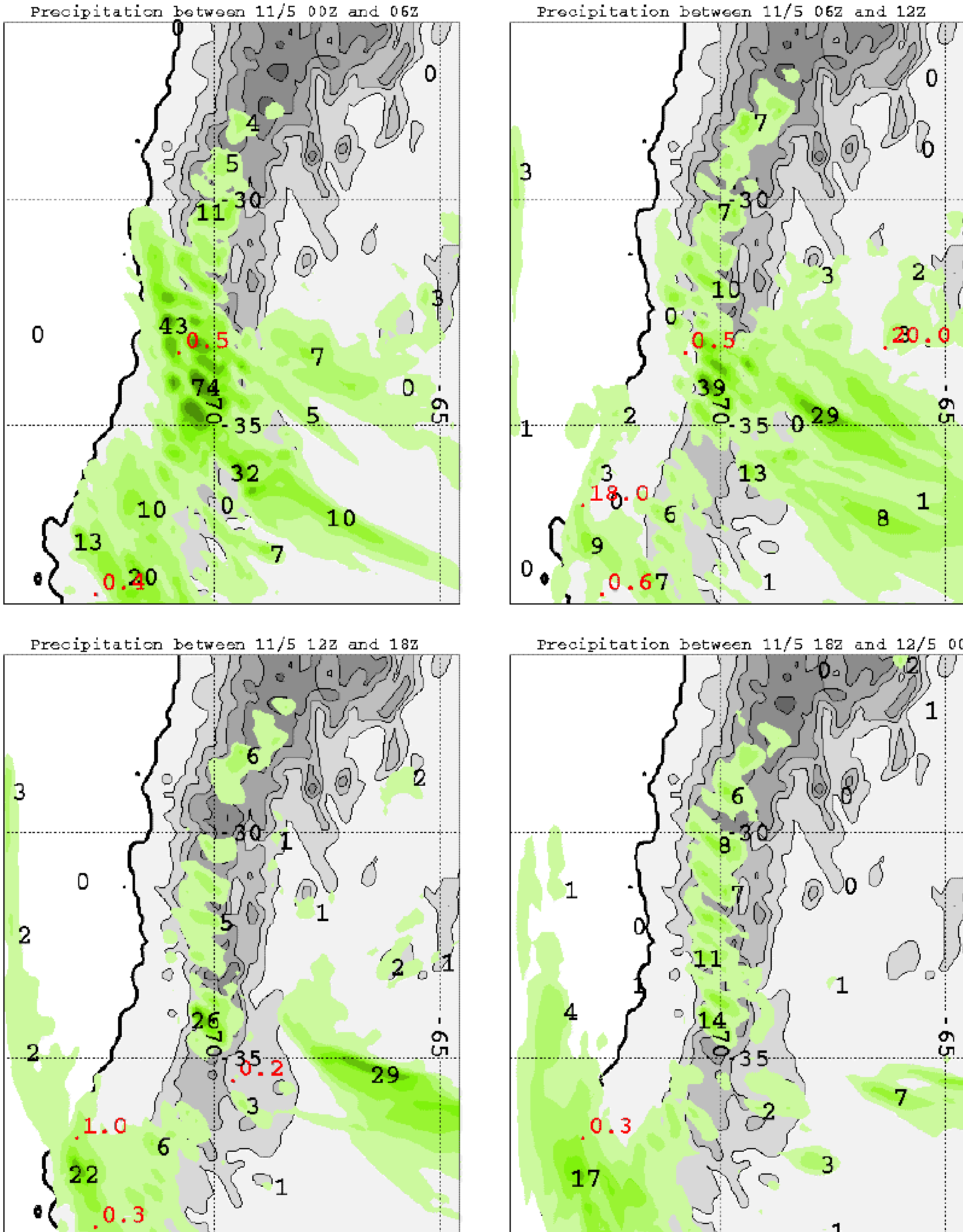


**Figure 2.4.** Maps of precipitation as simulated by HIRLAM during 11th May 1998. Numbers with decimals indicate observations; numbers without decimals indicate local maximum of model results. Unit: mm.

## 2.4. Results

May 1998 was a month with only weak wind speeds in the Santiago area. The WMO- observations show that this month was rainy in the southern part of the model area, around the cities Valdivia and Temuco. It was rather dry in the Santiago area, only two periods with rain, one in the middle of the month (11$^{th}$ May) and the other around 25$^{th}$ May. During both these periods the rain moved northward near the coast. In the northern part of Chile (inside the model area) May was a dry month. Figure 2.3 shows the simulated and observed cloud cover and the surface wind for four occasions during May 1998. On the 2$^{nd}$ and 16$^{th}$ May the winds are generally southerly to the west of the Andes with little cloud cover. The situation is different on the 9$^{th}$ and 23$^{rd}$ with northerly winds and more cloudiness coupled to the synoptic disturbances giving precipitation on the 11$^{th}$ and 25$^{th}$ in the Santiago area. The observed and simulated distribution of precipitation on the 11$^{th}$ is shown in Figure 2.4. Six-hour accumulated precipitation exceeding 30 mm is simulated on several mountain locations, which seems very high but still not unrealistic considering that there are observations showing six-hourly precipitation of up to 20 mm for the same period.

Table 2.1 shows the result of the statistical evaluation against surface synoptic stations for the whole month. RMS values for HIRLAM are somewhat lower than for ECMWF for 2-meter temperature and relative humidity. The bias is opposite with HIRLAM showing a positive bias while ECMWF shows a negative bias. For 10-meter wind speed and mean sea level (m.s.l.) pressure ECMWF shows slightly lower RMS and bias values than HIRLAM. For cloud cover the results for HIRLAM are significantly different from ECMWF showing a larger negative bias and larger RMS values. Cloud cover seems to be underestimated by HIRLAM.

**Table 2.1.** Calculated RMS and bias scores for synoptic stations for HIRLAM simulations and ECMWF analysis for May 1998.

| | **HIRLAM** | | **ECMWF** | | |
|---|---|---|---|---|---|
| | **RMS** | **Bias** | **RMS** | **Bias** | **No. of obs.** |
| 2 m temperature (°C) | 3.1 | 0.5 | 3.4 | -0.4 | 1823 |
| 2 m rel. Humidity (%) | 17.3 | 8.2 | 20.0 | -9.3 | 1676 |
| 10 m wind speed (m/s) | 2.6 | 0.8 | 2.2 | -0.4 | 1827 |
| m.s.l. pressure (hPa) | 1.5 | 0.3 | 1.0 | 0.0 | 1658 |
| cloud cover (octas) | 4.2 | -1.6 | 3.1 | -0.2 | 1806 |

The result of the statistical evaluation against the three sounding stations is shown in Table 2.2. The results for HIRLAM and ECMWF are comparable for temperature, relative humidity and geopotential while HIRLAM shows somewhat larger RMS and bias values for wind speed.

Figure 2.5 shows a comparison of observed and simulated cloud cover, wind speed and direction at 10 meter, temperature and relative humidity at 2 meter and mean sea level pressure for the synoptic station Pudahuel located at the airport of Santiago. The record is a bit difficult to interpret but some interesting features can be noted. The observations show that it is very humid at the station during nighttime. During many nights the relative humidity reaches 100 % and in these cases there is probably fog at the station. During the periods with high relative humidity the observed cloud cover is high, also during daytime. The HIRLAM simulation is not as humid as observed and also misses several periods with high observed cloud cover such as on the 5-7th, 10-11th, 19th and 26-28th. During these periods the differences between observed and simulated temperatures and wind speeds are also largest, while the agreement for all parameters are better in between. When the cloud cover is underpredicted the simulated temperatures become too high and the relative humidities become too low due to increased insolation. The simulated wind speeds tend to become too high at the same time probably caused by the simulated onset of thermally driven mountain-valley circulations.

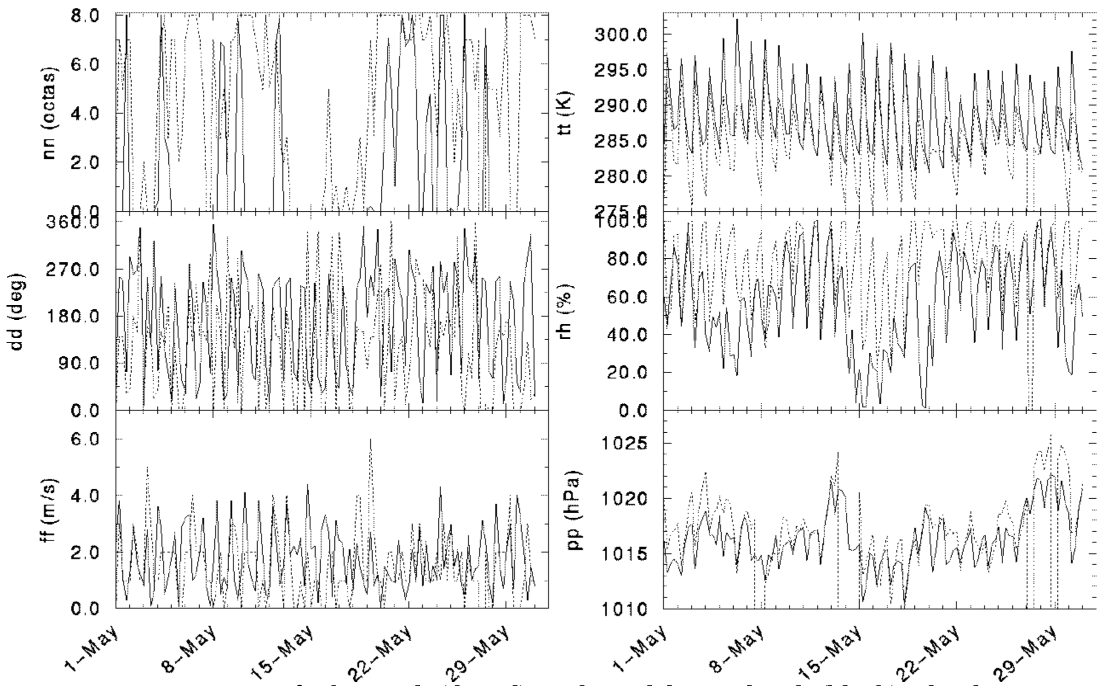


**Figure 2.5**. Time series of observed (dotted) and model simulated (black) cloud cover, wind direction, wind speed, 2 meter temperature, 2 meter relative humidity and surface pressure at Pudahuel (Table A.1)

**Table 2.2**. Calculated RMS and bias scores for sounding stations HIRLAM simulations and ECMWF analysis for May 1998.

| | HIRLAM | | ECMWF | | |
|---|---|---|---|---|---|
| **Wind speed (m/s)** | **RMS** | **Bias** | **RMS** | **Bias** | **No. of obs.** |
| 200 hPa | 5.5 | -2.4 | 3.6 | -1.1 | 58 |
| 300 hPa | 5.3 | -0.2 | 4.3 | -0.6 | 58 |
| 500 hPa | 4.9 | 0.3 | 3.6 | -0.2 | 57 |
| 700 hPa | 2.6 | -0.8 | 2.5 | 0.3 | 59 |
| 850 hPa | 3.0 | -0.9 | 2.4 | 0.2 | 58 |
| **Temperature (°C)** | | | | | |
| 200 hPa | 2.0 | 1.2 | 1.6 | 0.8 | 100 |
| 300 hPa | 1.0 | 0.3 | 0.9 | -0.2 | 106 |
| 500 hPa | 1.3 | 0.5 | 1.1 | 0.4 | 109 |
| 700 hPa | 1.5 | -0.6 | 1.7 | -0.9 | 108 |
| 850 hPa | 1.5 | -0.6 | 1.4 | -0.2 | 107 |
| **Relative humidity (%)** | | | | | |
| 200 hPa | 8.2 | 5.1 | 7.2 | 4.6 | 68 |
| 300 hPa | 12.2 | 7.9 | 10.2 | 5.8 | 68 |
| 500 hPa | 10.0 | 1.2 | 8.5 | -0.5 | 103 |
| 700 hPa | 8.3 | 0.2 | 7.6 | -0.1 | 89 |
| 850 hPa | 10.1 | 0.7 | 9.7 | -1.8 | 101 |
| **Geopotential (m)** | | | | | |
| 200 hPa | 15.8 | 8.3 | 11.7 | -2.2 | 102 |
| 300 hPa | 14.2 | 2.1 | 12.2 | -4.9 | 104 |
| 500 hPa | 10.3 | -4.3 | 8.9 | -4.3 | 107 |
| 700 hPa | 6.2 | -1.6 | 5.4 | -2.5 | 107 |
| 850 hPa | 6.0 | 2.7 | 5.3 | 1.9 | 105 |

Similar features can also be seen in the comparison with the stations in the network around Santiago. Four stations, which were judged to be representative for larger areas, were selected from the CENMA network. These are: La Platina (M01) which is located in an agricultural area south of Santiago; Lo Pinto (M04) which is located in the northern part of Santiago; Entel (M07) which is located at the top of a tower in central Santiago and Codigua (M11) which is located to the west, outside of the Santiago basin. Comparisons of observed and simulated time series of temperature at 2 meter and wind speed at 10 meter are shown in Figures 2.6 and 2.7. For wind direction at 10 meter (Figure 2.8) wind roses are shown instead of a time series because the time series plot is difficult to read in this case. Below each figure the mean, standard deviation, maximum and minimum value is also given. It should be noted that the data from Entel is taken at the top of a 100 m high tower. For this location data from the lowest model level (~35 m) in HIRLAM is used for comparison.

The comparison for temperature indicates a better agreement for La Platina, Lo Pinto and Codigua compared to Pudahuel, but still with a tendency towards overestimation. For Entel the simulation underestimates the temperature during nighttime. Comparison with the second model level would probably give a better agreement. Periods with the largest differences between observed and simulated temperature coincide with the periods with large differences in observed and simulated cloud cover noted at Pudahuel. The comparison for wind speed shows that HIRLAM generally overestimates the wind speed, especially during the first half of the month. Periods with the largest differences between observed and simulated wind speed coincides again with the periods with large differences in observed and simulated cloud cover noted at Pudahuel. Wind roses are compared in Figure 2.8. When looking at these it should be kept in mind that the wind direction for surface stations is strongly influenced by topography. The resolution used in the HIRLAM simulation is not high enough to put the topographic features in exactly the right position in relation to the stations and this impacts on the simulation results. The differences that are seen can be related to topographic effects combined with the effect of periods with too strong simulated thermally driven flows.

Periods with favorable meteorological conditions for high concentrations of air pollution in Santiago have been identified according to the classification by Rutllant and Garreaud (1995). Rutllant and Garreaud identify two main patterns: Type A, which corresponds to the onset of a coastal low in central Chile moving southward along the coast. A depressed subsidence inversion prevails ahead of the low and leads to suppressed vertical mixing. Type BPF, which is a prefrontal condition ahead of a weak and often occluded front, which slows down or becomes stationary when reaching central Chile. The classification for May indicates that A-type episodes occurred during 16-19$^{th}$ and May 30$^{th}$ – June 3$^{rd}$ while B-type episodes occurred during 5-8$^{th}$ and 22$^{nd}$ (CENMA, 1998). The first A-type episode appears to be well simulated with a good correspondence with observations. The behavior for the Second A-type episode is difficult to judge since it extends beyond the simulation period. The first B-type episode coincides with a period of underestimated cloud cover and too strong simulated wind speeds and is not well predicted by HIRLAM. The second B-type episode on the 22$^{nd}$ appears however to be better simulated.

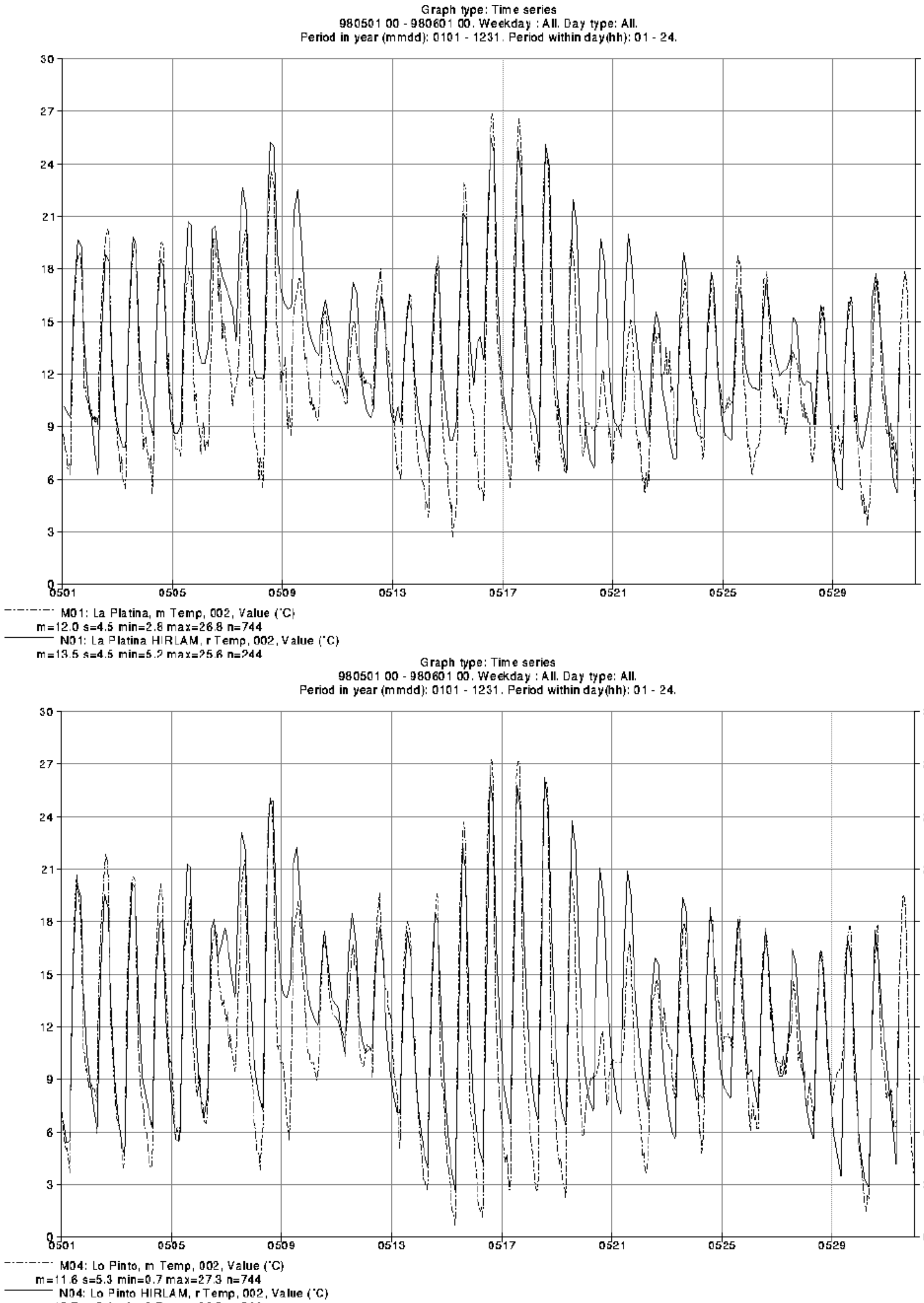


**Figure 2.6 a.** Model calculated (full line) and observed (dash-dotted line) temperature at two meter at the stations La Platina (M01) and Lo Pinto (M04). Units: °C.

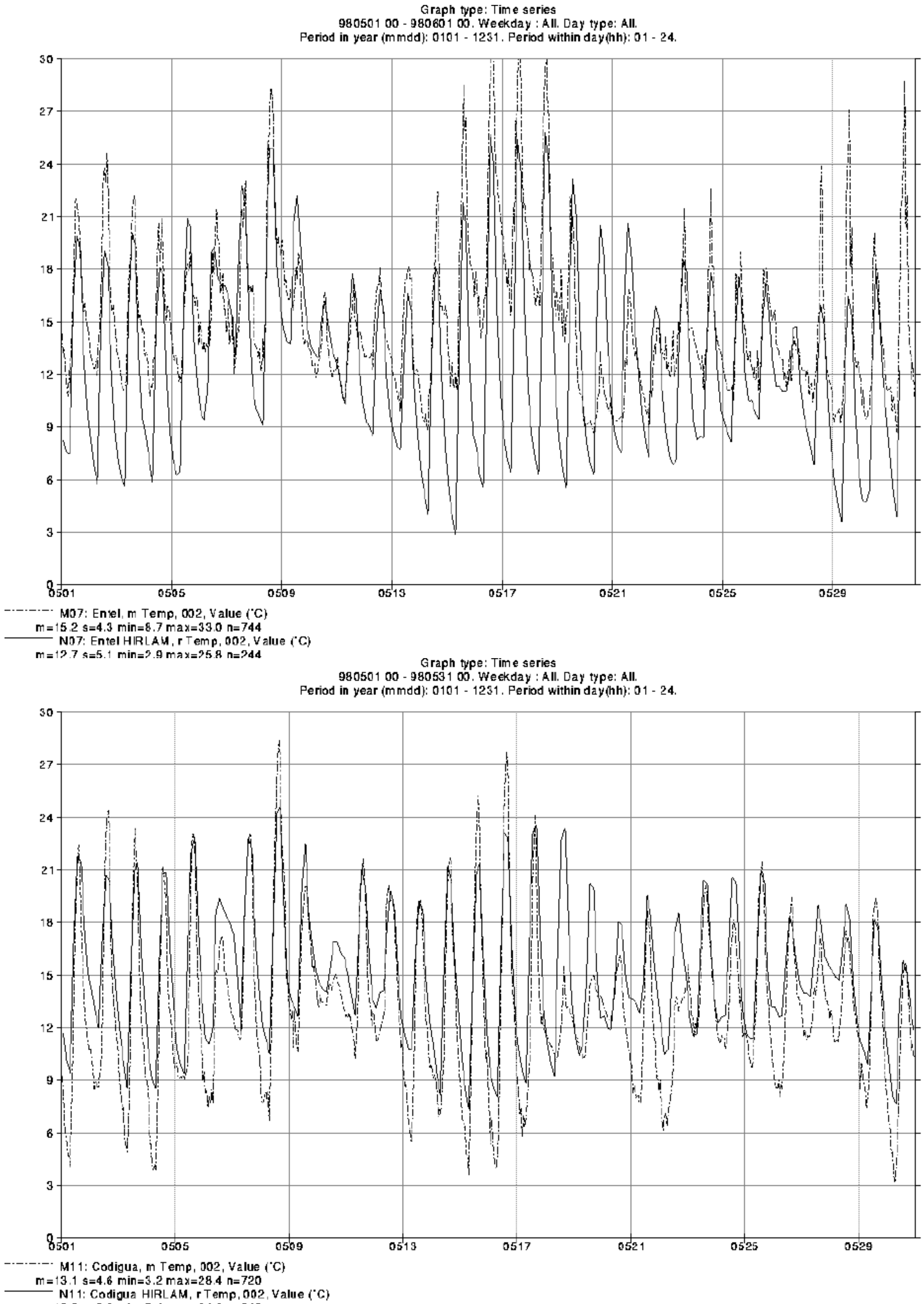


**Figure 2.6 b.** Model calculated (full line) and observed (dash-dotted line) temperature at two meter at the stations Entel (M07 100 m) and Codigua (M11). Units: °C.

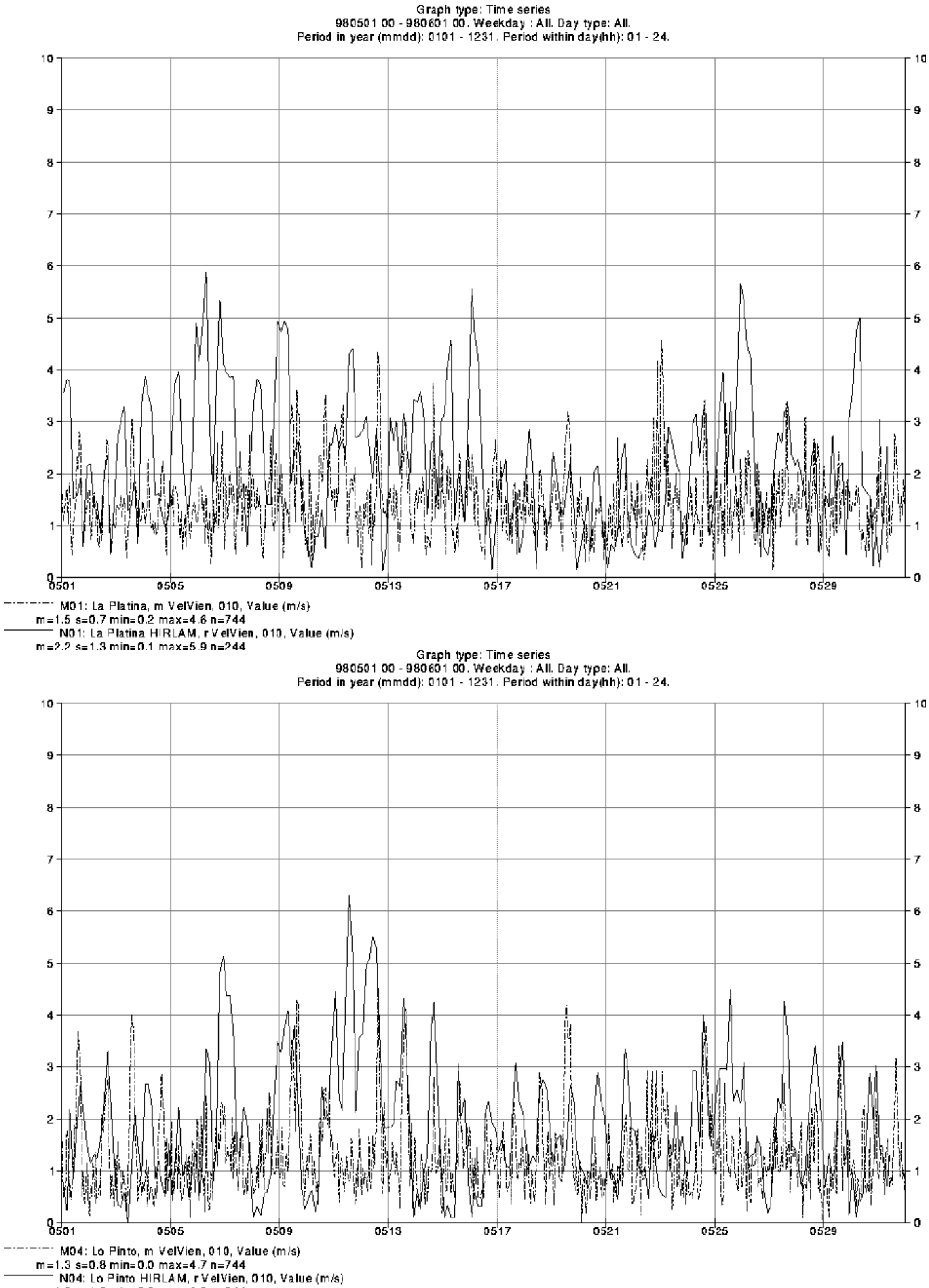


**Figure 2.7 a.** Model calculated (full line) and observed (dash-dotted line) wind speed at 10 meter at the stations La Platina (M01) and Lo Pinto (M04). Units: m/s.

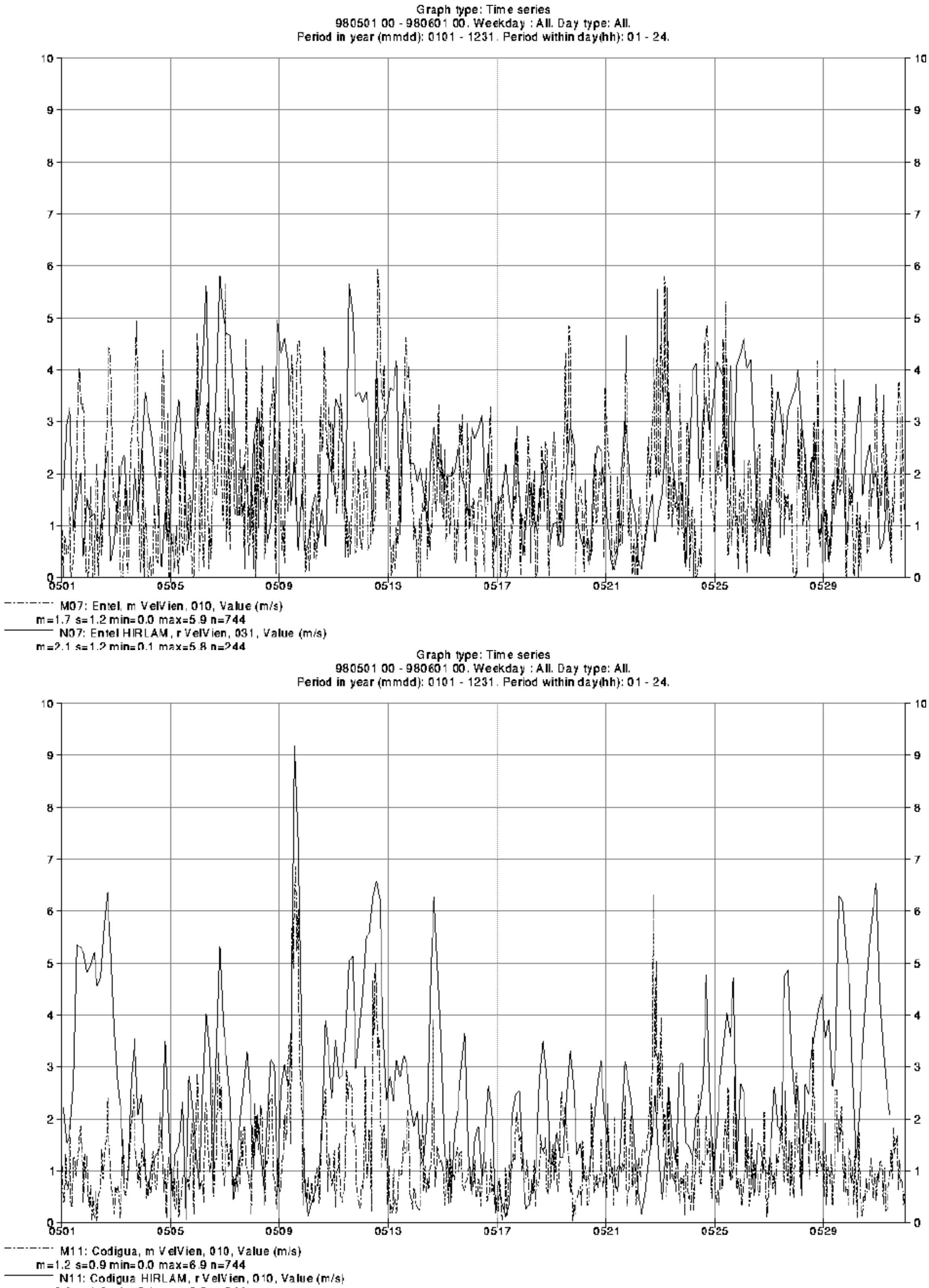


**Figure 2.7 b.** Model calculated (full line) and observed (dash-dotted line) wind speed at 10 meter at the stations) Entel (M07 100 m) and Codigua (M11). Units: m/s.

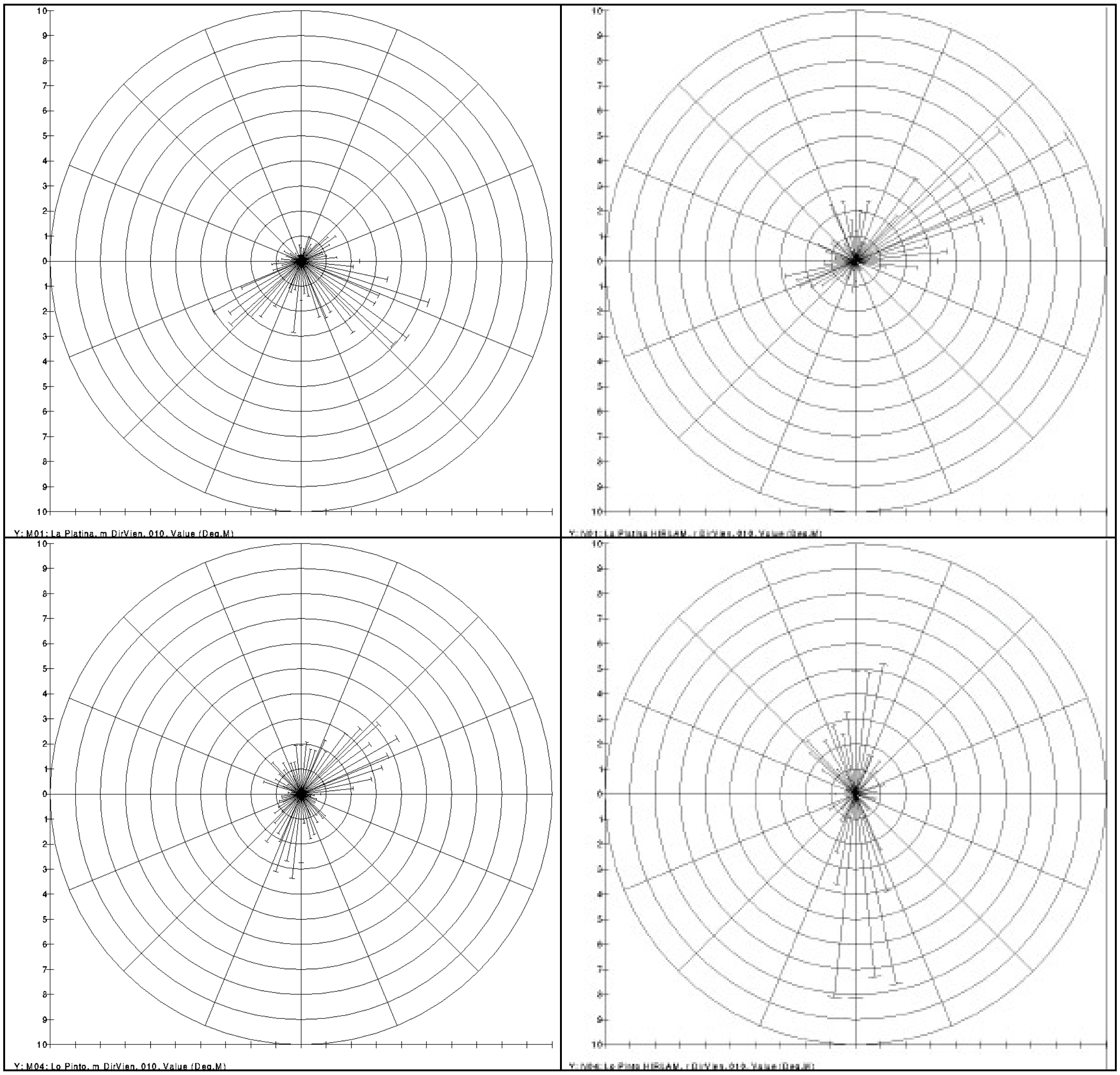


**Figure 2.8 a.** Observed (left) and calculated (right) average wind roses at 10 meter at the stations Lo Pinto (M04 and La Platina (M01). Units: % per sector.

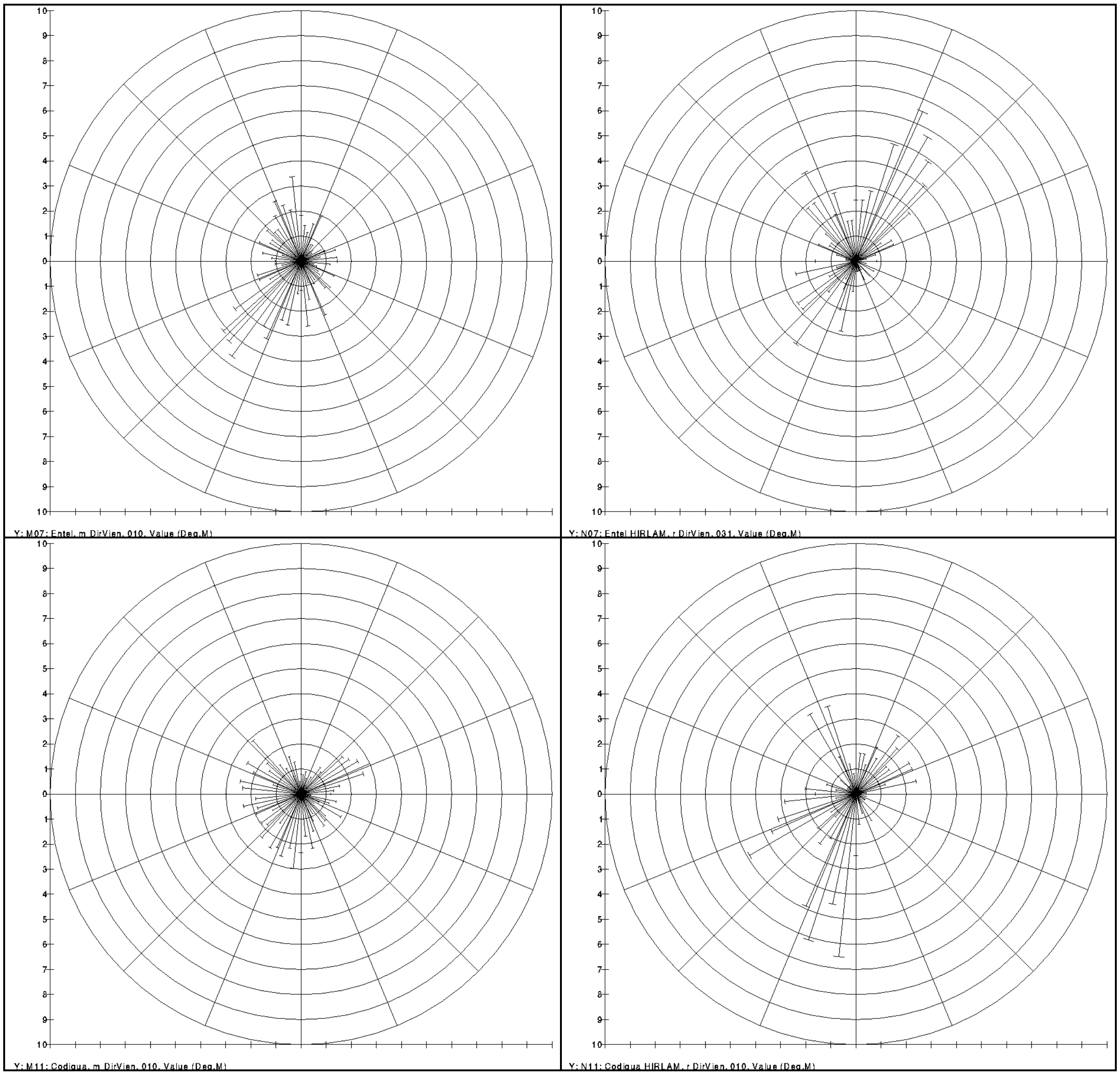


**Figure 2.8 b.** Observed (left) and model calculated (right) wind roses at 10 meter at the stations Entel (M07), and Codigua (M11). Units: % per sector.

## 2.5. Discussion and summary

Two month-long meteorological simulations using HIRLAM over Chile have been evaluated so far. The simulation of January 1998 was very successful and provided a good description of the distinct diurnal variations of the wind and temperature in the Santiago region although details in the surface wind direction were not resolved. Also on a larger scale the simulation was good and the statistical evaluation against synoptic meteorological stations actually indicated a slight improvement compared to the ECMWF analysis. January 1998 was a summer period with little cloudiness in the Santiago area and thermally driven circulation with up and down-slope winds along the Andes. The simulation for May 1998, which is a fall/winter month, is not as good as for January 1998. The fall/winter in the Santiago region is characterized by cloudy weather and low wind speeds. HIRLAM tends to produce too little cloudiness and too strong winds for several periods, especially during the first half of May 1998. When the cloudiness is underpredicted this affects the stability of the lower atmosphere resulting in stronger vertical mixing during daytime which increases surface wind speeds. The daytime surface temperature also increases leading to the onset of thermally driven circulations in the simulations which tends to increase the surface wind speeds further during daytime.

Several tests were made in order to try to improve the simulation results. An updated version of HIRLAM was used for the simulations presented here compared to January 1998. The version used is HIRLAM 4.7.0. This version has options for a modified condensation scheme named STRACO (Sass et al., 1999). The main difference between this scheme and the one used in the simulation for January 1998 is that it is numerically more stable due to an implicit formulation and that convection is allowed to start at higher altitudes in addition to surface level. Version 4.7.0 of HIRLAM also has options for a new turbulence scheme named CBR (Cuxart et al., 2000) based on a turbulent kinetic energy approach. These new schemes were tested to see if they could improve numerical stability problems related to condensation processes and to improve the simulation of low level clouds.

So far all comparisons between observations and simulations for the winter months show that the model simulations predict too little moisture near the surface. Attempts were made to increase low level moisture by changing the climatological soil moisture content prescribed for lower layers in the soil to the maximum 0.020 $kg/m^2$, but the predicted low level moisture was still too low.

The model also appears to simulate too much precipitation in the fall/winter situations, especially in the mountain area. It should be kept in mind though that we do not really know how much precipitation is falling in the mountains during the winter months, because of the sparse observations. Changes have been made in the calculation of horizontal diffusion of humidity near the ground, but this did not have a strong effect on the simulated precipitation in the mountain areas. One should realize that the steep topography in Chile is difficult to handle with the convection schemes currently used in HIRLAM and that we are running the model at a horizontal resolution, which is higher than these schemes were originally designed for.

Prediction of clouds and precipitation in general and low-level clouds in particular is a common problem for current numerical weather prediction (NWP) models. Difficulties with prediction of low level clouds are evident also for HIRLAM as well as for other models for European conditions. New turbulence and condensation schemes are currently tested for HIRLAM but further tuning is needed probably also coupled to a higher vertical resolution in the lower part of the atmosphere.

The results presented here clearly indicate that current NWP models are able to capture many of the meteorological features that are important for describing the dispersion of air pollutants over Chile. Improvements in the simulation of meteorological conditions for future studies over Chile should be possible to achieve using updated versions of HIRLAM and by tailoring the model resolution to the application in question.

# 3. DISPERSION MODELING (MATCH)

**G. Olivares and L. Gallardo**
*National Commission for the Environment, Chile*

The dispersion of pollutants depends on the physical and chemical characteristics of the tracers, the emission rates and the meteorological conditions. The emissions and the meteorological conditions vary both in time and space. Also, the tracers suffer chemical and physical transformations. Hence, a modeling tool must be evaluated for different meteorological conditions and emission scenarios. Here we present an evaluation of the HIRLAM-MATCH system for May 1998. This is an analysis of a fall scenario, which must be considered complementary to the summer scenario earlier presented (CONAMA-SMHI, 1999).

The May 1998 period was chosen because of the severe air quality episodes observed in the area during that period (CENMA, 1998) and the availability of information for validation purposes. At this stage, we focus our evaluation in the dispersion of oxidized sulfur over Central Chile (See Figure 3.1). We consider two oxidized sulfur reservoirs: the sulfur dioxide reservoir ($S\text{-}SO_2$) and the sulfate reservoir ($S\text{-}SO_4$).

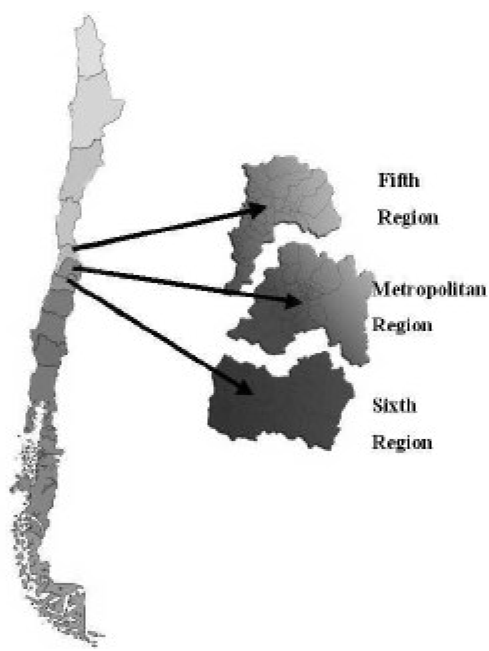


**Figure 3.1.** Map of Central Chile. Political regions for which the model is applied, i.e., 5$^{th}$, 6$^{th}$ and Metropolitan, are outlined.

The results presented hereafter are intended to primarily assess which features of the May 1998 high-concentration episodes are reproduced by the model. Also a first and rather rough assessment of the partitioning between the $S\text{-}SO_2$ and $S\text{-}SO_4$ reservoirs is presented. This issue is important since Central Chile, particularly the Santiago Metropolitan area, suffers a severe air pollution problem by inhalable particles, especially fine particles (≤2,5 µm), which to a significant extent are associated with secondary sulfate aerosols (CONAMA-RM, 1997). In order to assess better the model results, first we analyze the observations and identify the main features of the air quality situation for May 1998. Then we check whether the model reproduces these patterns. All the meteorological simulations used correspond to the HIRLAM simulations for May 1998 earlier described (Cf. Section 2).

### 3.1. Air Quality Data Analysis

Sulfur dioxide ($SO_2$) is the only sulfur compound regularly monitored at several sites in Central Chile. Sulfate has been only sporadically monitored in connection with specific short-term campaigns using different measuring techniques. A specific measuring campaign intended to assess, among other things, secondary aerosols, was performed during winter 1999 in Santiago (Oyola pers. comm.). During that campaign simultaneous measurement of $SO_2$ and sulfate as well as nitrogen oxides and nitrate were made. These data will be especially analyzed in a future report. These data are important as they help us assessing the partitioning between $SO_2$ and sulfate. In the meantime, we will focus our analysis of air quality data on $SO_2$.

The stations and the availability of $SO_2$ data during May 1998 for the model domain are summarized in the Table 3.1. The location of the monitoring stations is illustrated in Figure 3.2. Figure 3.2 also shows the topography of the area as seen by the model. Most of the Santiago stations are located at around 500 m above sea level, except Las Condes (EMM), which is at ca. 700 m of altitude. The Puchuncaví network consists of four stations, which are located at about 200 to 300 m of altitude. The Chagres network consists of four stations placed at about 500 to 600 m. The Caletones network stations are located at various altitudes: Machalí (mML) is around 500 m, Coya Población (mCP) at 750 m, Coya Club de Campo (mCY) at 1000 m, Colón (mCO) at 2000 and Sewell (mSW) at 2800 m. The estimates of the altitudes have been obtained from standard geographical maps (IGM, 1988). The administrators of these stations are indicated in Table 1. These are: the Metropolitan Environment Health Service (SESMA), the Corporación Nacional del Cobre de Chile (CODELCO Chile, the National Copper Corporation of Chile), the Agricultural Service (SAG), Puchuncaví Air Quality Surveillance System (SVAP) and Chagres Air Quality Surveillance System (SVACH). The data have been kindly provided by the National Commission for the Environment at Santiago Metropolitan Office (CONAMA-RM), at Rancagua in the Sixth Region (CONAMAVI), and at Valparaíso in the Fifth Region (CONAMA V). Also SAG at Quillota has kindly provided data from the networks that survey the power plants in the 5$^{th}$ region.

In addition to the data described above, we also consider information obtained through a cooperative program between Chile and Switzerland. This program, known as “COSUDE project”, aims at a diagnostic analysis of air quality at five cities in Chile, among them Valparaíso (33º05'S, 71º40'W), Viña del Mar (33º01'S, 71º33'W) and Rancagua (34º10'S, 70º46'W). COSUDE has provided information about monthly means of $SO_2$ at these urban areas using a passive sampler technique (Jadrijevic et al., 1999).

In the following, the observations for the different political regions included in the model domain are summarized and discussed, i.e., the Metropolitan area of Santiago, the 5$^{th}$ and 6$^{th}$ Regions (Cf. Figure 3.1 and Figure 3.2).

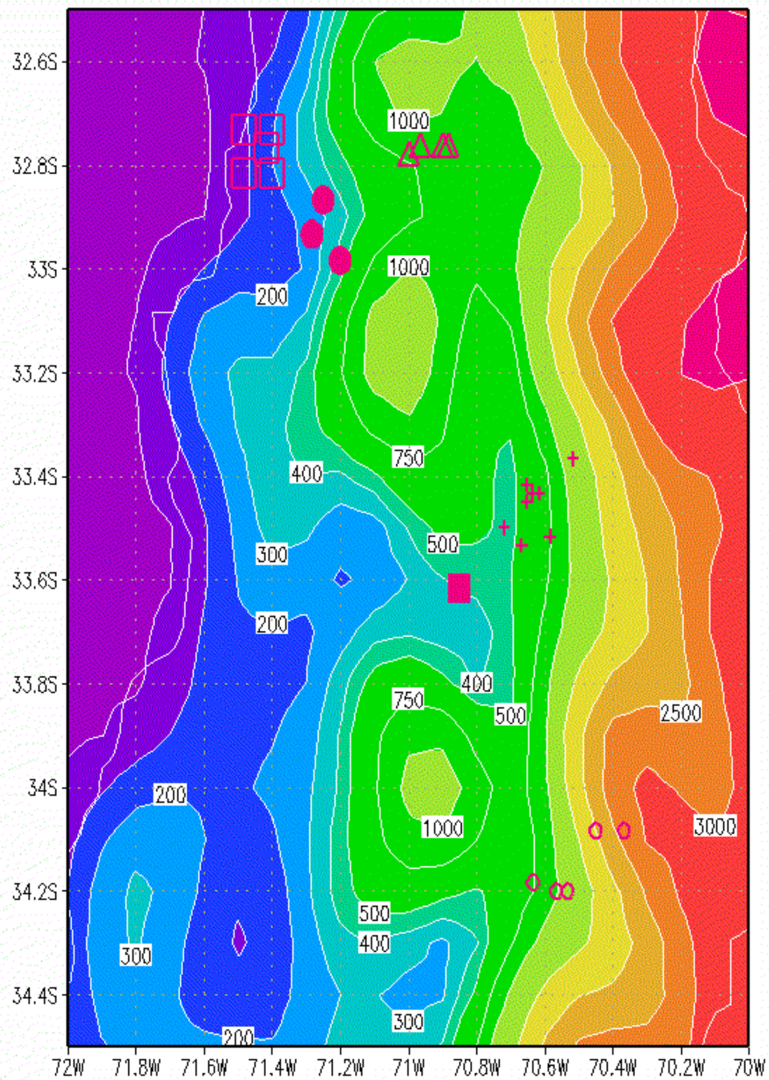


**Figure 3.2.** Location of the stations considered in the model evaluation. The different networks are indicated with different marks: crosses correspond to the Santiago network, circles indicate the sixth region network, filled circles are for the Quillota network, open squares correspond to the Ventanas network, open triangles indicate the Chagres network and the filled square correspond to the Talagante station. Altitude isolines for 200, 300, 400, 500, 750, 1000, 2500 and 3000 meters are shown.

**Table 3.1.** $SO_2$ concentration data for May 1998. Also, data for May 1999 have been included for the Quillota area. Sources: CONAMA-RM, SESMA, CONAMA V, SAG and CONAMA VI.

| Station Code | Name | Lat (S) | Lon (W) | Availability (%) | Administrator | Remarks |
|---|---|---|---|---|---|---|
| | | | **Metropolitan Region of Santiago** | | | |
| EML | La Florida | 33º31’ | 70º35’ | 66 | SESMA | Hourly data available until May 22nd |
| EMD | Parque O'Higgins | 33º27’ | 70º39’ | 100 | SESMA | Hourly data |
| EMM | Las Condes | 33º22’ | 70º31’ | 100 | SESMA | Hourly data |
| EMQ | El Bosque | 33º32’ | 70º40’ | 99 | SESMA | Hourly data. May 11th is missing |
| GMA | Cerrillos | 33º30’ | 70º43’ | 68 | SESMA | Hourly data. From May 19th to 27th is missing |
| EMB | Seminario | 33º26’ | 70º38’ | 100 | SESMA | Hourly data |
| EMF | Av La Paz | 33º25’ | 70º39’ | 100 | SESMA | Hourly data |
| R20 | DOAS | 33º26’ | 70º37’ | 69 | SESMA | Hourly data available until May 22nd |
| SS4 | Talagante | 33º37’ | 70º51’ | 96 | SESMA | Some hourly data missing |
| | | | **Sixth Region** | | | |
| MCO | Colón | 34º05’ | 70º27’ | 100 | CODELCO | Hourly data |
| MCP | Coya Población | 34º12’ | 70º32’ | 100 | CODELCO | Hourly data |
| MCY | Coya C. Campo | 34º12’ | 70º34’ | 100 | CODELCO | Hourly data |
| MML | Machalí | 34º11’ | 70º38’ | 100 | CODELCO | Hourly data |
| MSW | Sewell | 34º05’ | 70º22’ | 100 | CODELCO | Hourly data |
| | | | **Fifth Region** | | | |
| | | | Quillota | | | |
| BQI | Bomberos Quillota | 32º52’ | 71º15’ | | SAG | Hourly data May 1999 |
| CSP | Cajón San Pedro | 32º56’ | 71º17’ | | SAG | Hourly data May 1999 |
| UCV | Agro-UCV | 32º59’ | 71º12’ | | SAG | Hourly data May 1999 |
| | | | Puchuncaví | | | |
| PCV | Puchuncaví | 32º44’ | 71º24’ | 100 | SVAP | Monthly Avg. |
| MTN | Los Maitenes | 32º46’ | 71º25’ | 100 | SVAP | Monthly Avg. |
| GDA | La Greda | 32º44’ | 71º29’ | 100 | SVAP | Monthly Avg. |
| VAG | Valle Alegre | 32º49’ | 71º24’ | 100 | SVAP | Monthly Avg. |
| SUR | Estación Sur | 32º49’ | 71º29’ | 100 | SVAP | Monthly Avg. |
| | | | Chagres | | | |
| MGT | Sta. Margarita | 32º46’ | 70º53’ | 100 | SVACH | Monthly Avg. |
| CMP | Lo Campo | 32º46’ | 70º54’ | 100 | SVACH | Monthly Avg. |
| CAT | Catemu | 32º46’ | 70º58’ | 100 | SVACH | Monthly Avg. |
| ROM | Romeral | 32º47’ | 71º00’ | 100 | SVACH | Monthly Avg. |

### *3.1.1. Metropolitan area of Santiago*

The monthly averages (Table 3.2) show that the maximum concentration of $SO_2$ is reached over the central axis of the city (EMF, EML) while the minimum occurs outside the urban area (SS4). A west-east gradient is observed from Talagante (SS4) to Seminario (EMB)-La Paz (EMF) and an east-west gradient are observed from downtown towards Las Condes (EMM). On a monthly average basis, no significant north-south gradient is observed. Notice the large variability of the data as expressed in the standard deviation. This is related to the strong diurnal cycle of the observed concentrations since the monthly average is calculated with the hourly data. Smaller standard deviations than those shown in Table 3.2 result when considering the daily averages, which filter out the diurnal cycle.

**Table 3.2.** Monthly average concentrations for the Santiago stations in May 1998. Unit: μg $SO_2/m^3$.

| Station | EMB | EMD | EMF | EML | EMM | EMQ | GMA | R20 DOAS | SS4 |
|---|---|---|---|---|---|---|---|---|---|
| Monthly Average | 29 | 28 | 30 | 29 | 13 | 20 | 28 | 26 | 1.6 |
| Standard Deviation | 26 | 27 | 25 | 34 | 10 | 28 | 25 | 22 | 2.4 |
| Maximum | 280 | 348 | 307 | 351 | 63 | 372 | 249 | 263 | 27 |
| Minimum | 3 | 3 | 3 | 5 | 3 | 3 | 5 | 1 | 0.1 |
| Nº Obs. | 743 | 743 | 743 | 490 | 743 | 736 | 505 | 512 | 713 |

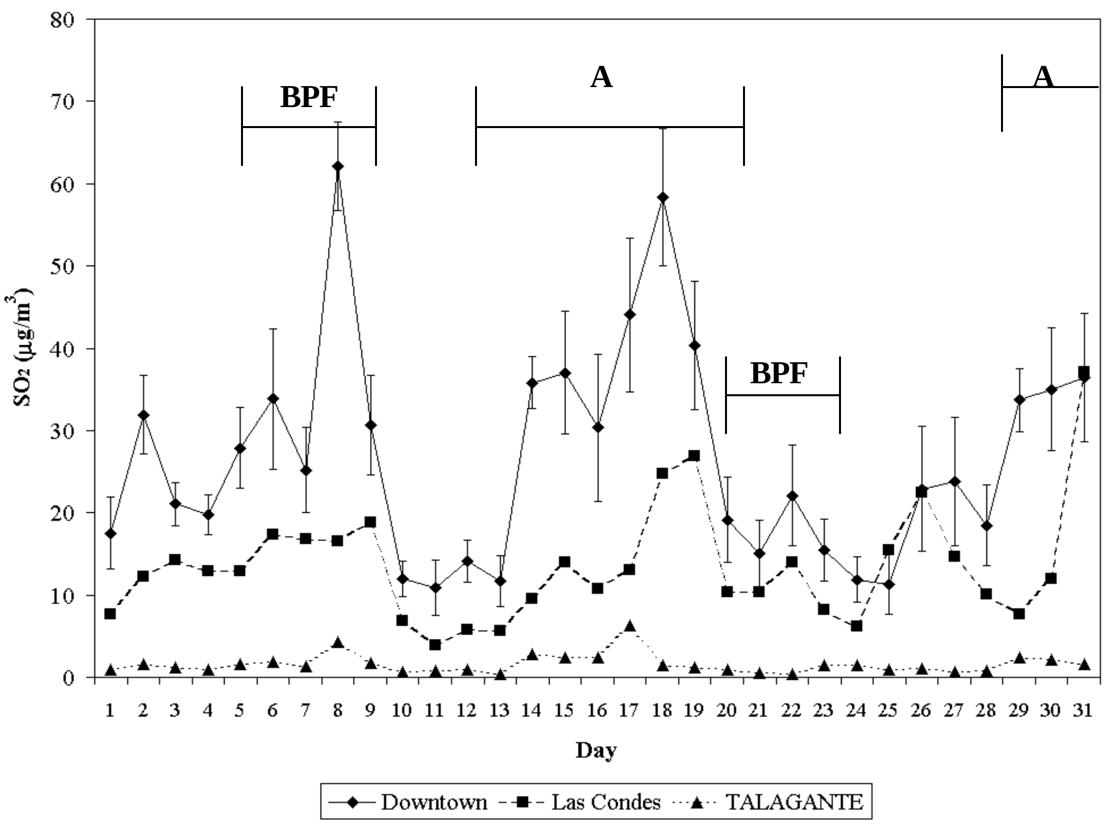


**Figure 3.3**. Measured $SO_2$ concentrations daily average for the downtown stations (EMD, EML, GMA, EMB, EMF, and EMQ), Las Condes (EMM) and Talagante (SS4) for May 1998. Also, episode periods are indicated. $SO_2$ concentration in μg/m$^3$.

According to the daily average values, one can distinguish three groups of stations. A first group that includes the downtown stations (EMD, EML, GMA, EMB, EMF, and EMQ) and two single-station groups. The former single-station group is that of Las Condes in the eastern bound of the basin. The second one is that of Talagante to the west of the basin. Several maxima occur simultaneously at all stations indicating that either a common source or similar meteorological conditions affect the stations in those occasions. The two largest maxima occur on May $8^{th}$ and May $18^{th}$. On these days a similar concentration is reached (60 $\mu g/m^3$) over Santiago but the variance among the stations is larger on the $18^{th}$ than on the $8^{th}$ as seen in the standard deviation indicated in Figure 3.3. The report prepared by the National Center for the Environment for the Metropolitan office of CONAMA (CENMA, 1998) indicates that the former episode (around May $8^{th}$) corresponds to a prefrontal situation or a BPF configuration as described by Rutllant and Garreaud (1995). It also indicates that the latter episode corresponds to a low-level through or an A configuration according to the same classification. It is worth noticing that these meteorological configurations define $SO_2$ episodes that last differently. The former configuration (BPF, May $5^{th}$ to $8^{th}$) triggers an episode that lasts only one day and the $SO_2$ concentrations rise from about 25 $\mu g/m^3$ to 60 $\mu g/m^3$ (average for the downtown stations) and then go back to 30 $\mu g/m^3$ in only 3 days (See Figure 3.3). During the A type episode, the concentrations rise from 30 $\mu g/m^3$ ($15^{th}$) to the maximum of 60 $\mu g/m^3$ ($18^{th}$) in three days, taking another two days to get down to ca. 30 $\mu g/m^3$. This is consistent with the time span of the meteorological configurations. The BPF configuration lasts 3 days and the A type episode lasts 5 days (CENMA, 1998). For the A type configuration, although the stable meteorological conditions prevail longer, the advection of humid air from the coast leads to a decrease in the $SO_2$ concentrations on May $19^{th}$.

The EMM station, located on the eastern boundary of the basin, shows the lowest $SO_2$ concentrations inside the urban area, except May $24^{th}$ through $26^{th}$ when the EMQ reaches the lowest values. At Talagante (SS4), the same features observed in downtown Santiago are present but with concentrations that are about ten times lower. The variations as well as the periods of maximal concentration at Talagante generally coincide with those observed at the urban stations.

The diurnal cycles are clearly different for the EMM and SS4 stations as compared to the rest of the Santiago network (See Figure 3.4 a). These two stations show a midday maximum much broader than for any of the other stations. In the case of Las Condes, the midday maximum could be associated with the advection of $SO_2$-rich air from the sources located in the city. In fact, due to the geographical location of this station, a defined diurnal cycle of the winds with up-slope winds during daytime exists. This brings to Las Condes air that has been exposed to sources located downtown Santiago. Similar arguments suggest that air exposed to the downtown sources should be transported to Talagante during the evening and nighttime hours. Hence, in absence of significant local sources, one would expect that Talagante should experience maximum concentrations during nighttime. However, the maximum occurs during the early afternoon. This indicates that other sources than Santiago’s may contribute to the mid-afternoon maximum at Talagante. One such a contributing factor could be associated with long-range transport from the copper smelters outside the Santiago basin at hours of maximum vertical mixing. The effect of other sources, located to the west of Talagante, cannot be disregarded though. It is worth noticing that very low values of $SO_2$ (<2 $\mu g/m^3$) are reported for nighttime at Talagante. In fact, these values are close to the detection limit for standard instruments, which makes it difficult to draw any definite conclusions from the Talagante measurements for nighttime conditions.

The rest of the stations within the basin show two maxima, one at 9 - 10 a.m. and other at 4 - 8 p.m. The intensity of these two maxima is different on each location but the afternoon maximum is always larger and broader than the morning maximum. Two factors may explain these maxima. Firstly, one associated with transportation sources, and secondly, one associated with point sources located in Southern Santiago. In fact one would expect morning and late afternoon maxima in connection with the morning and evening rush hours (transportation sources). This could explain the location of the maxima and, to some extent, the different time span as the evening rush-hour lasts typically longer than the morning rush hour. However, as shown in Figure 3.4 b, the evening maximum appears earlier in the southern most location (EMQ) and later in the northern most locations (EMF). This, in connection with the southerly wind component that prevails in the late afternoon at these sites, leads us to think that sources in southern Santiago may partly explain the different timing and width of the afternoon maximum at different locations. In fact, south of Santiago a significant $SO_2$ source is located, namely a molybdenum smelter. This hypothesis is consistent with the trajectory analyses presented by CONAMA-RM (Flores et al, 2000).

A weekly variation is also apparent in the observations (See Figure 3.5). A distinct maximum takes place on Friday. This pattern is common for all stations except for Las Condes (EMM). A similar behavior is seen when looking at a longer time-period from March to May 1998. The reported emissions do not show, however, any distinct weekly variation for $SO_2$. A similar, but larger in magnitude, weekly variation is observed for carbon monoxide (CO) and particulate matter (Cassmassi, 1999). If the reported emissions are correct, we are lead to think that an accumulation of $SO_2$ occurs along the week. This could be the case if the average removal rate in the basin during the period is smaller than the emission rate. However, as we only consider one month of data any definite conclusions about the weekly variation can be drawn at this stage.

In summary, the observed $SO_2$ concentrations reach highest values along the central north-south axis of the city while the lowest values are observed outside the urban area. There are the two distinct maxima in the observations during this period, the first one at the $8^{th}$ and the second one at the $18^{th}$, which are apparent on every station. These two maxima are related to two different meteorological conditions. The former corresponds to a BPF meteorological configuration and the latter to an A type configuration. These configurations last differently but result in similar $SO_2$ concentrations. There are different diurnal variations in the $SO_2$ concentrations for the stations in the downtown area and for those outside this area. The downtown diurnal variation of the $SO_2$ concentration shows a morning maximum around 9 a.m. and an afternoon one around 5 p.m. These two maxima may be explained firstly by transportation sources that have a strong diurnal variation and secondly by $SO_2$-rich air advection from the south where there is a large point source. The stations in the suburbs, EMM and SS4, show a different diurnal variation one from another. Advection of air exposed to downtown sources appears to be a major contributor to the observed diurnal cycle at Las Condes. Long-range transport and vertical mixing at hours of maximum insolation may explain the observed diurnal variation at Talagante. A weekly variation is also apparent from the observations but not from the reported emissions. This suggests that on average $SO_2$ accumulation may occur in the basin along the week.

a)

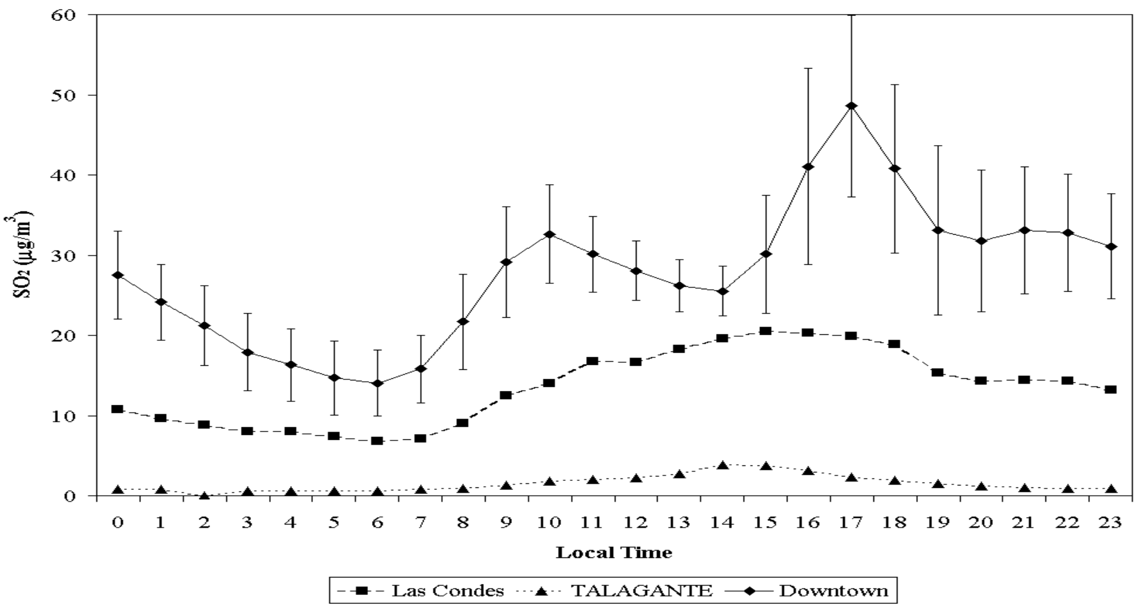


b)

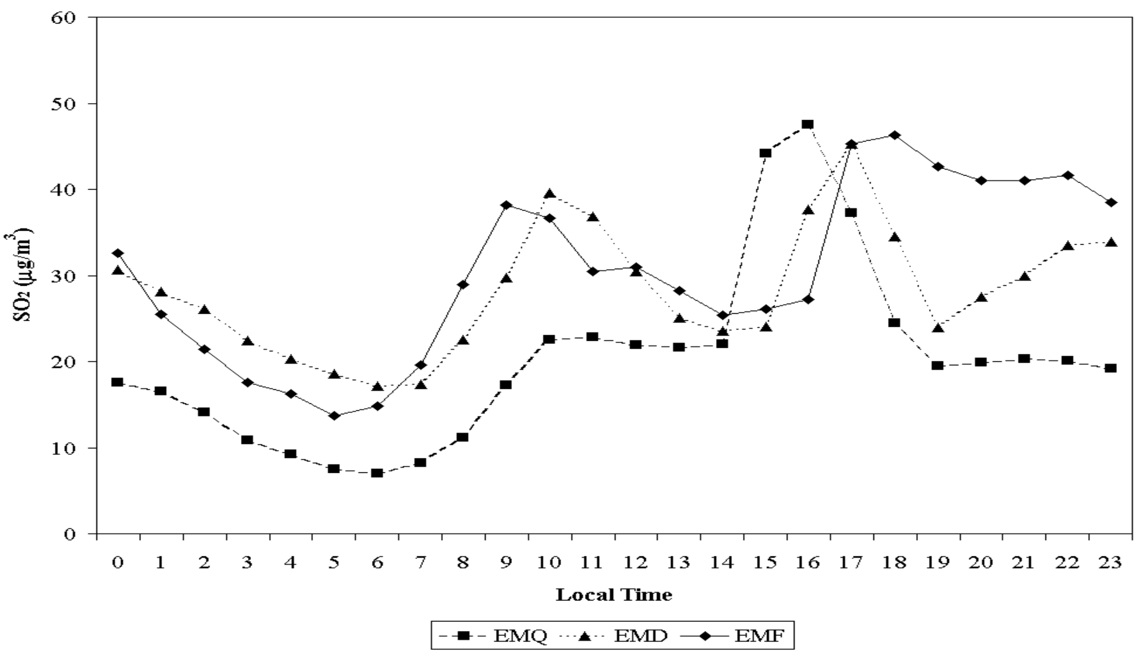


**Figure 3.4**. Diurnal variation for the Santiago stations for May 1998: a) Downtown average, Las Condes and Talagante; b) EMQ, EMD and EMF. $SO_2$ concentration in µg/m$^3$.

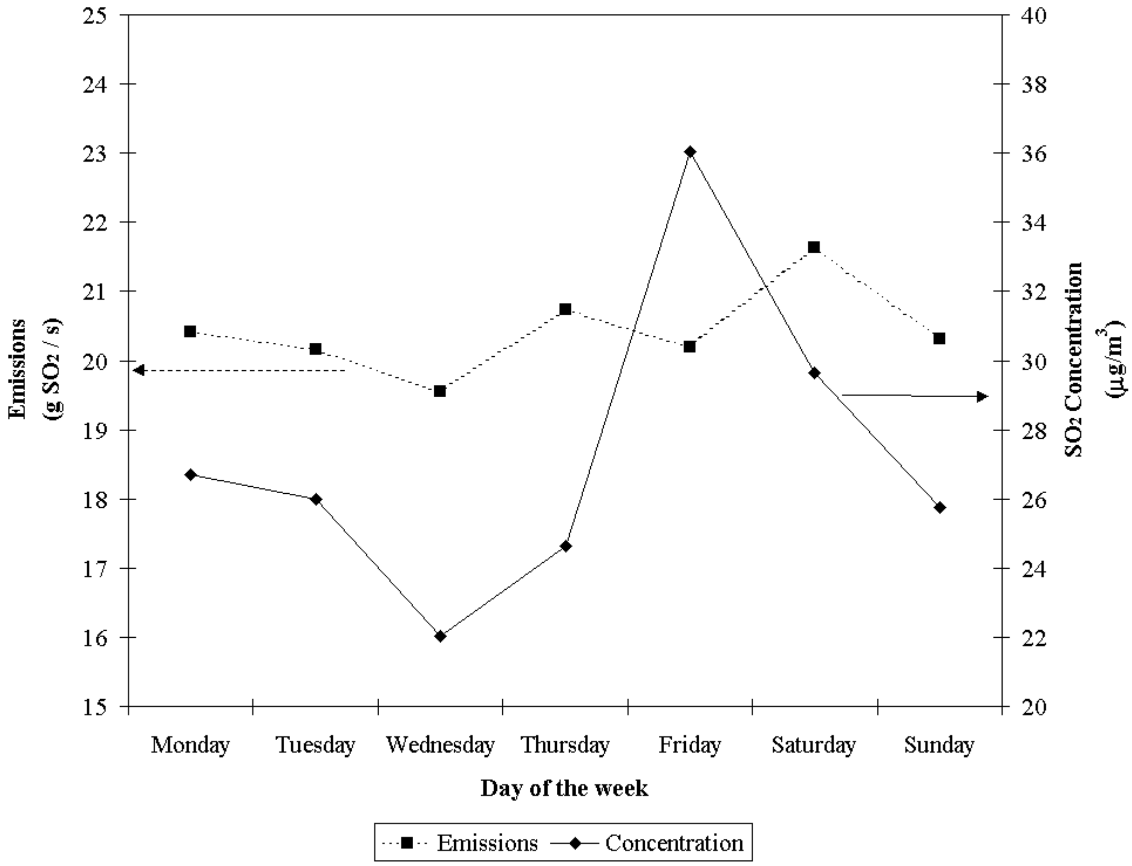


**Figure 3.5**. Weekly variation of $SO_2$ concentration and emission for the Santiago stations for May 1998. $SO_2$ concentration in $\mu g/m^3$. Emissions in g $SO_2$/s.

### *3.1.2. 6^th^ Region*

Three stations are particularly considered for the 6th region in our analysis: Coya (ca. 1000 m.a.s.l.) at the top of a hill, Coya Población (ca. 750 m.a.s.l.) by southern slope of the same hill and Machalí (ca. 500 m.a.s.l.) to the west end of this valley. The other two stations are too close to the source and therefore they do not provide insights relevant for our purposes. In addition to these data we review the observations provided by the COSUDE project.

The monthly averages (See Table 3.3) show decreasing concentrations downhill from the Caletones Copper Smelter (Machalí, mML station). The levels reached on these stations in the 6th region are about five to ten times larger, excluding the Colón (mCO) station, than those reached in Santiago. The large standard deviations reported are related to the strong diurnal variation of the observations. The COSUDE data indicate monthly average values between 30 and 110 $\mu gSO_2/m^3$ for the Rancagua area. The highest values are observed nearby Machalí. This suggests the impact from the copper smelter placed up-hill (Caletones). This is to some extent corroborated by an apportionment analysis of the COSUDE data given by Koutrakis (1999). That analysis shows that on an annual basis an smelter's emissions are responsible for almost 30% of the observed inhalable ($PM_{10}$) and fine particles ($PM_{2.5}$), i.e., secondary aerosols, downtown Rancagua. However, according to the same study, the contribution from smelters placed in the urban areas cannot be disregarded.

**Table 3.3.** Monthly averages for the 6$^{th}$ region stations. Unit: $\mu gSO_2/m^3$

| Station | mCO | mCP | mCY | mML |
|---|---|---|---|---|
| Monthly Average | 1900 | 120 | 480 | 74 |
| Std. Dev. | 4000 | 159 | 843 | 186 |
| Min | 10 | 10 | 10 | 10 |
| Max | 35000 | 1500 | 6600 | 1170 |
| Nº Obs. | 743 | 743 | 743 | 743 |

In the daily $SO_2$ averages, the Caletones stations (Coya, Coya Población and Machalí) show similar variations but a couple of days earlier than those observed at the Santiago stations (See Figure 3.6). This is particularly noticeable for the A type episode of the 18$^{th}$. The BPF episode is not as evident for the stations in the 6$^{th}$ region as for the Santiago stations. This difference in timing of the 18$^{th}$ maximum may be partially explained by the fact that even though the meteorological conditions are similar both in the Santiago basin and in the 6$^{th}$ region, the Caletones emissions affect first the 6$^{th}$ region and then the Metropolitan region. However, the effects of local sources in Santiago cannot be ruled out.

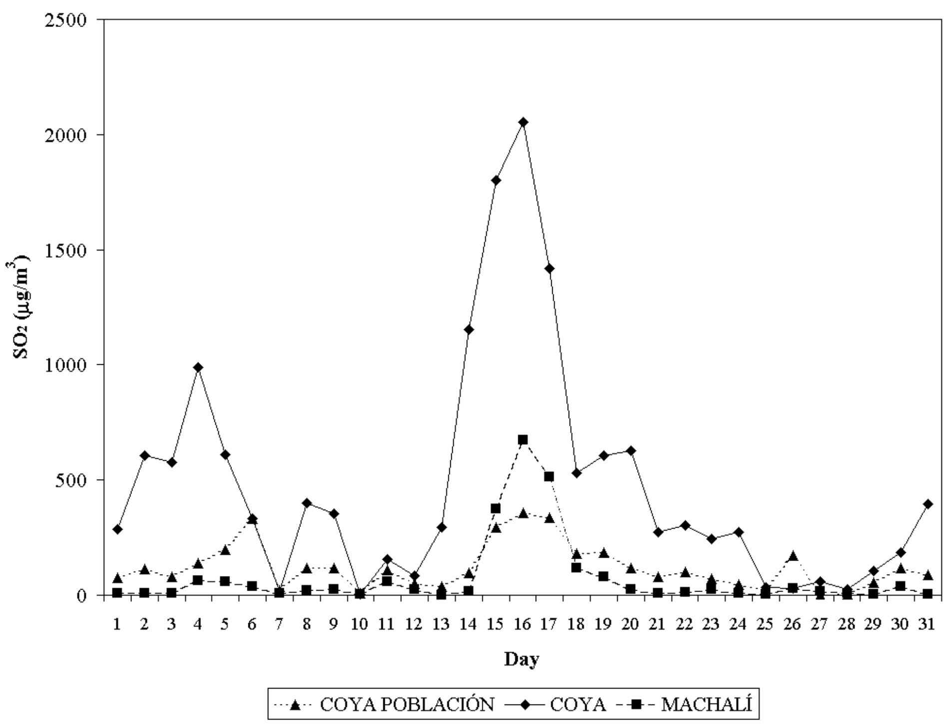


**Figure 3.6.** Daily averages for selected stations in the 6$^{th}$ region for May 1998. $SO_2$ concentration in $\mu g/m^3$.

The Coya station shows a diurnal variation that reflects the impact of the Caletones smelter, with highest concentrations during nighttime and lowest concentrations during daytime (Figure 3.7). At the other two stations there is a mid-morning or noon maximum and a mid-afternoon minimum in the concentrations. At Machalí there is a slight increase in the concentrations during the night. We hypothesize that during the night there is a down-slope advection of $SO_2$-rich air from the smelter whose effects are different at the three stations due to the differences in altitude. The Caletones plume directly affects the station at the top of the hill (Coya). At Machalí and Coya Población the impact is possibly inhibited during nighttime by the presence of a strong vertical layering in the canyon where these stations are located. At Machalí and Coya Población, the effect of the nighttime down-slope advection becomes apparent only once the vertical mixing becomes effective in the mid-morning and noon hours. However, especially at Machalí, the effects of local sources cannot be ruled out.

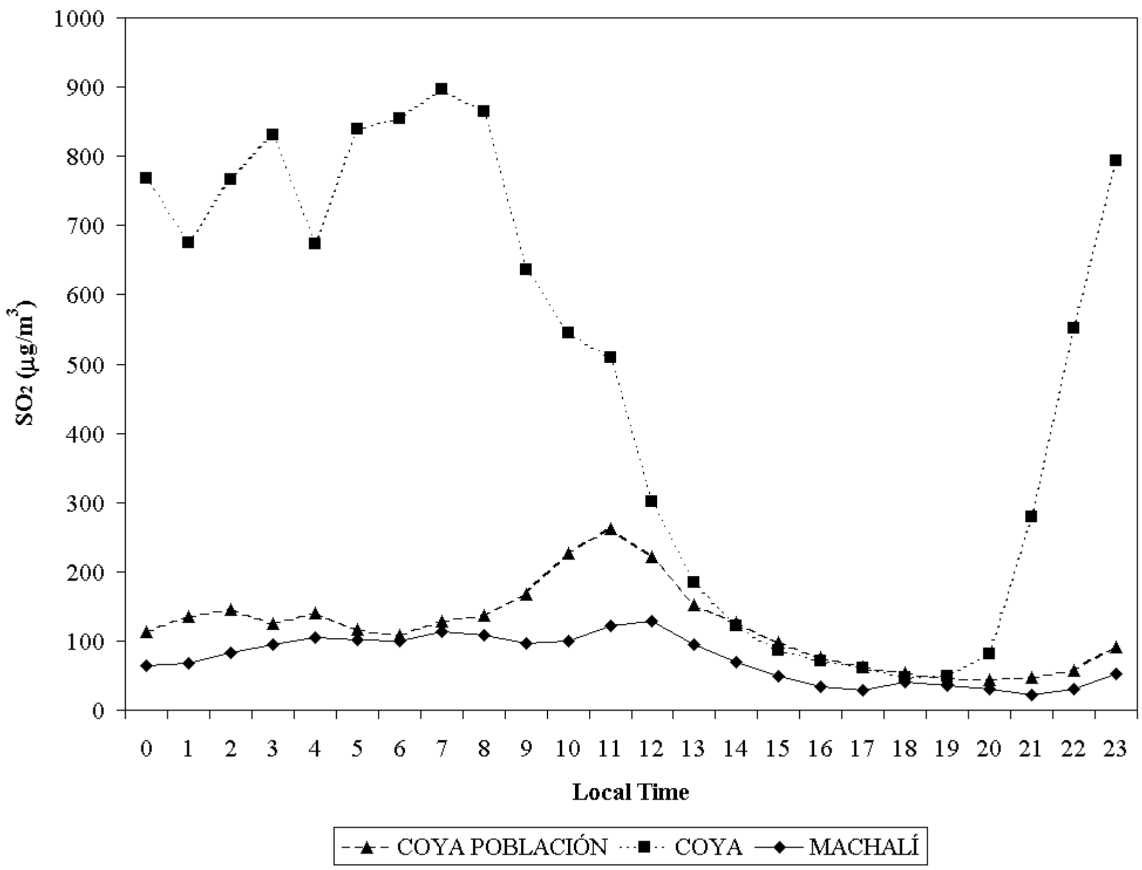


**Figure 3.7.** Diurnal variation for May 1998 at selected stations in the 6th region. $SO_2$ concentration in $\mu g/m^3$.

In summary, the $SO_2$ concentrations measured in the sixth region network show higher concentrations near the Caletones copper smelter and lower concentrations down in the valley. Also the observations in Rancagua indicate the impact from the Caletones smelter. The maximum observed concentrations appear at all three stations (mCP, mCY, mML) and coincide with the A type configuration but two days earlier than in the Santiago network. This is may be because the emissions from Caletones copper smelter impact before over the sixth region stations than in Santiago. A strong diurnal cycle is apparent at the Coya station with highest $SO_2$ concentrations during nighttime and lowest concentrations during daytime. This reflects the direct impact of the Caletones plume over mCY station. The other two stations (mML and mCP) show a different diurnal variation with relatively low concentrations during nighttime, which we hypothesize are related to the stable conditions in the valley that inhibits the impact of the Caletones plume during the night. At Machalí and Coya Población a distinct noon maximum is apparent when the vertical mixing becomes effective.

### *3.1.3. 5$^{th}$ Region*

The information available in the fifth region for May 1998 is scarce. There are no observations on an hourly basis reported for May 1998. Only monthly averages are available. For three of these stations hourly data is available for May 1999. In lack of better information, we therefore use the May 1999 hourly data as a surrogate for fall conditions at these locations. See Table 3.1 for details.

For May 1998 the monthly averages indicate a north-south gradient with highest concentrations at Estación Sur (32º49'S, 71º29'W) and lowest concentrations at La Greda (32º44'S, 71º29') (See Table 3.4). The Chagres stations show, except Santa Margarita, similar monthly average $SO_2$ concentrations of about 30 $\mu g/m^3$ among the stations. These values are generally lower than those observed at Ventanas, which may be partially due to the different emission rates of these copper smelters. Other differences may arise from the differences in the location of the stations relative to the location of the source. Also differences in the overall ventilation and vertical mixing conditions in each area may play a role.

The COSUDE data for the main urban areas of the fifth region (Viña del Mar and Valparaíso) show monthly average values between 10 and 50 $\mu gSO_2/m^3$. In this case it is difficult to establish the relative impact of the urban sources and the Ventanas's smelter. According to Koutrakis (1999) an smelter's emissions explain, on an annual basis, nearly 50% of the $PM_{2.5}$ measurements downtown Viña del Mar and only 6% of it downtown Valparaíso. Moreover, especially in Valparaíso, the contribution from local sources appears to be significant.

For the Quillota area a distinct diurnal cycle with maximum concentrations in the afternoon is apparent from the 1999 observations (See Figure 3.8). The sea-breeze circulation at the coast is perhaps topographically enhanced by the presence of the Aconcagua valley, which has an east-west orientation near the coast. This would result in westerly winds during the day, which may advect $SO_2$-rich air from the Ventanas-Chilgener area, and easterly winds during the night, which may bring relatively clean air over the area.

**Table 3.4.** Monthly averages and maximum $SO_2$ concentration reported for stations in the 5th Region (No other statistics are reported). Bomberos Quillota, Cajón San Pedro and Agro-UCV have hourly information for May 1999. Unit: μg $SO_2/m^3$.

| Station Code | Station | Monthly Average | Maximum |
|---|---|---|---|
| | Quillota area | | |
| mQT | Bomberos Quillota | 17 | 90 |
| CSP | Cajón San Pedro | 16 | 120 |
| UCV | Agro-UCV | 13 | 130 |
| | Ventanas network | | |
| mPV | Puchuncaví | 70 | 260 |
| MTN | Los Maitenes | 130 | 290 |
| GDA | La Greda | 14 | 120 |
| VAG | Valle Alegre | 39 | 120 |
| SUR | Estación Sur | 130 | 430 |
| | Chagres network | | |
| MGT | Sta. Margarita | 59 | 160 |
| CMP | Lo Campo | 34 | 90 |
| mCM | Catemu | 28 | 70 |
| ROM | Romeral | 29 | 90 |

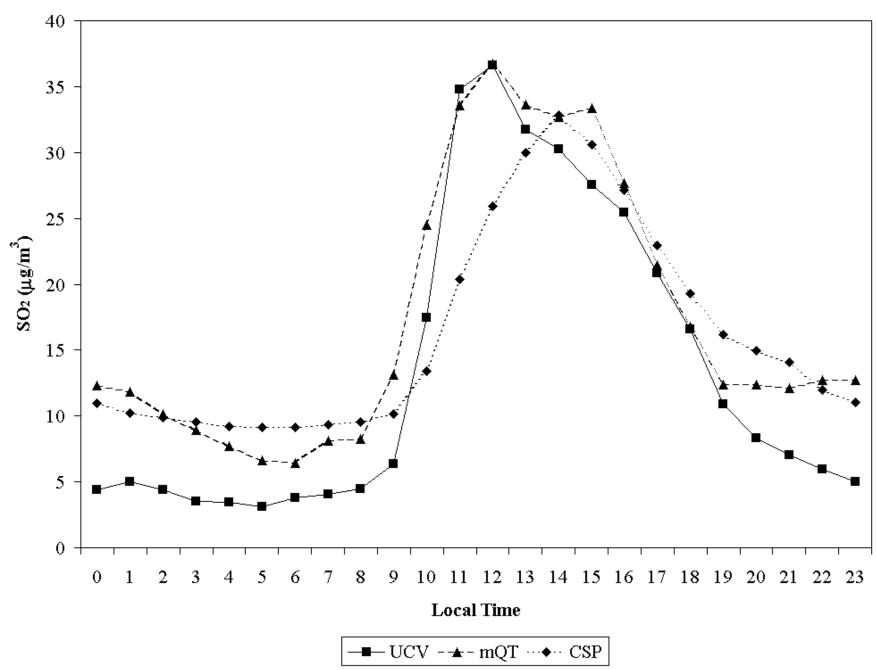


**Figure 3.8.** Diurnal variation for the 5th Region stations. $SO_2$ concentration in μg/m$^3$.

In summary, for the period of May 1998, the $SO_2$ concentration monthly averages indicate a north-south gradient near the Ventanas copper smelter. Near the Chagres smelter the concentrations are consistently lower than in Ventanas being that partially because of the different emission rates of these two sources and because local ventilation characteristics of each area. The main urban areas of the $5^{th}$ region probably suffer the impact of the Ventans's copper smelter too, however its magnitude is difficult to assess. For the Quillota area the diurnal cycles observed in 1999 show an afternoon maximum, which, we speculate, may be the effect on the Ventanas plume dispersion of the topographically enhanced sea-breeze circulation by the Aconcagua valley.

## 3.2. Simulations

### *3.2.1. Model set-up*

The model set-up is identical to that applied for the summer case (See CONAMA-SMHI, 1999 for details). Only the emissions have been changed (See Table 3.5). Recall that the model does not include a sink term for $SO_2$ due to fog or in-cloud deposition. Only the removal due to precipitation events is considered.

**Table 3.5**. Total emissions for May 1998. Source CONAMA. Unit $gSO_2/s$

| | January 1998 | May 1998 |
|---|---|---|
| **Santiago** | **420** | **470** |
| **Megasources** | | |
| Polpaico | 230 | 230 |
| Chagres | 250 | 400 |
| Ventanas | 2000 | 1500 |
| Caletones | 24000 | 22000 |
| **Regional Emissions** | **100** | **100** |
| **Total** | **27000** | **24700** |

### *3.2.2. Results*

*a) Regional distribution and partitioning of sulfur*

As well as for January 1998 (CONAMA-SMHI, 1999), the large copper smelters located in the area dominate the oxidized sulfur burden outside the urban areas (See Figure 3.9). The modeled horizontal distribution of $SO_2$ for May 1998 is similar to that simulated for January 1998 but the simulated concentrations are larger in the May than in the January scenario. The main reason for this is that the atmospheric conditions are typically more stable during fall (particularly in May 1998) than during summer resulting in higher concentrations of oxidized sulfur in the boundary layer.

The pattern of relative contribution of the copper smelters to the sulfur burden in Central Chile during May 1998 is similar to that of January 1998, i.e., only a smaller (<10%) fraction of the sulfur burden outside the urban areas, and above the boundary layer (not shown here) is explained by urban emissions. The predominance of the copper smelters is larger in the May scenario than in the January scenario.

January 1998 May 1998

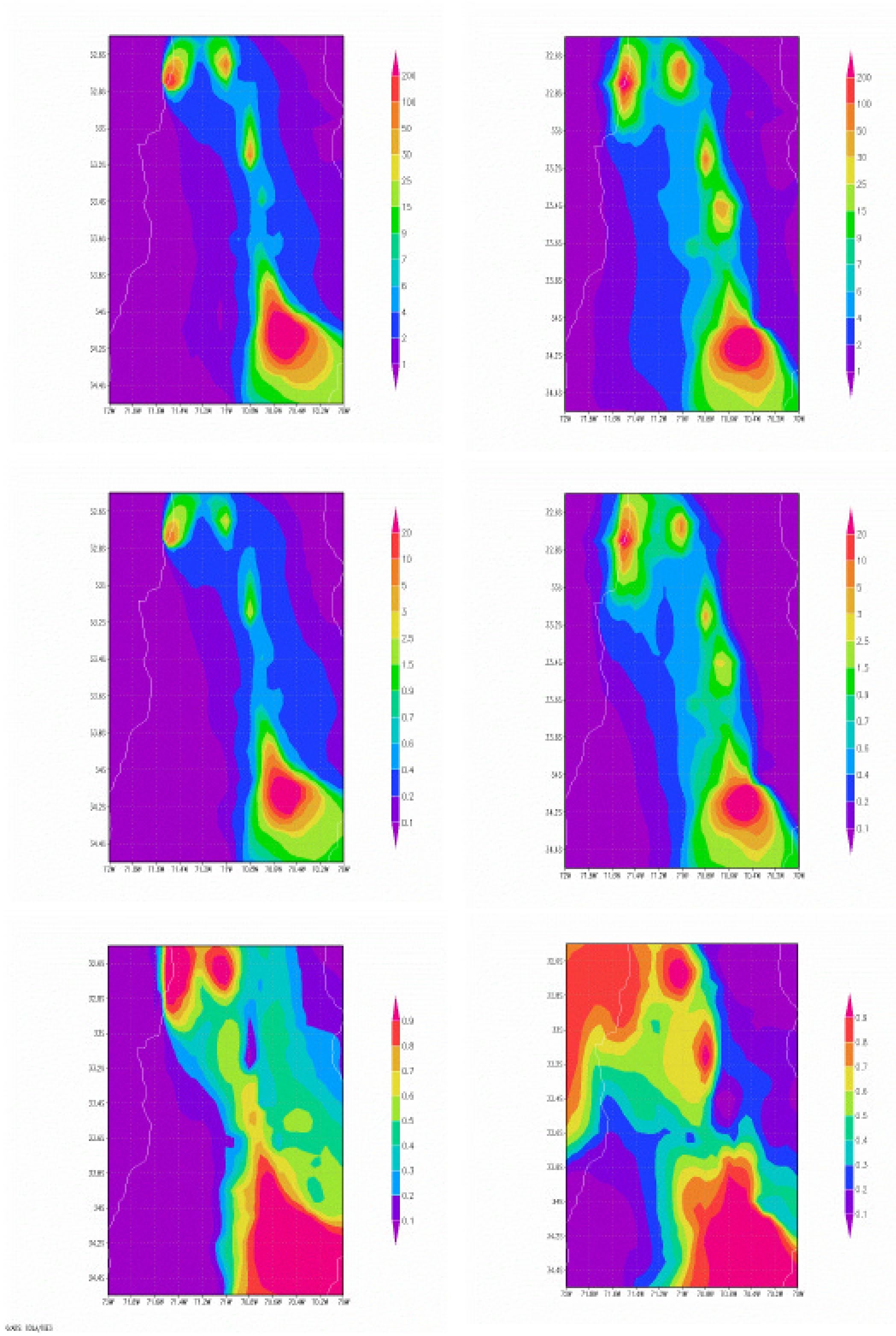

**Figure 3.9.** Simulated monthly averaged oxidized sulfur distributions. $SO_2$, $SO_4$ ($\mu g/m^3$) and smelters relative contribution to $S\text{-}SO_2 + S\text{-}SO_4$ in the upper, middle and lower panels respectively.

For the January scenario we could not assess the partitioning between sulfur as $SO_2$ and sulfur as sulfate due to the lack of sulfate observations for that period. We are slightly better off for the May scenario since monitoring campaigns reported by Artaxo (1998) do contain some indications of the actual partitioning between $SO_2$ and sulfate. In fact, Artaxo (1998) reports seasonal averages of the total sulfur content measured in aerosol filters for inhalable particle matter ($PM_{10}$) during winter 1998 (May-August) at several locations in Santiago and surrounding areas. Namely at Parque O'Higgins, Las Condes and Talagante, i.e., downtown, eastwards and westwards of Santiago city respectively. These measurements provide an upper limit for sulfate in the boundary layer at these locations during fall and winter 1998. Taking these observations as surrogates for sulfate we build up an observed partitioning, which we compare with the model results (See Table 3.6). According to this, the calculated partitioning at Parque O'Higgins (EMD) is roughly consistent with the observed one. Larger discrepancies are found at Las Condes (EMM) and Talagante (SS4). However, as shown later, the sulfur concentrations at these stations are not satisfactorily simulated due to shortcomings in the emission inventories and the wind field simulations. Although we are aware that the available observations for May 1998 do not put a strong constrain on the sulfur partitioning, the consistency of the results lead us to think that the model simulations are not far off from the actual sulfur partitioning. We will address the partitioning issue in an upcoming report in which measurements with higher temporal resolution will be analyzed.

Another interesting feature that can be identified by analyzing the partitioning between the two sulfur reservoirs represented in the model is the following. Namely that in connection with the A type configuration an enhanced subsident regime is established, which brings down air from the upper levels to the boundary layer. The upper-air is in turn relatively rich in sulfur that has been transported from the copper smelters. Thus, according to the model calculations, an episodic impact of the copper smelters occurs when an A type configuration is established. This is illustrated in Figure 3.10. There we show the twenty-four hours moving average of sulfate over $SO_2$ simulated ratios. Also the smelters contribution to the total sulfur in the boundary layer is shown. From these series one can see that an increase in the relative amount of sulfate is apparent from the $14^{th}$ to the $20^{th}$, which according to the model, coincides with the increase in the impact of the megasources both in $SO_2$ and sulfate. This coincides with the decrease in the boundary layer height as a consequence of the A type configuration (See Figure 3.12).

**Table 3.6**. Comparison between the model and the observed sulfur partitioning expressed as g $SO_4$-S/ g $SO_2$-S. The observations are seasonal averages (May through August 1998) and the model results are monthly averages (May 1998). Notice that the observed values are derived from the total sulfur content in inhalable particles ($PM_{10}$).

| **Station** | **Obs** $SO_4$-S/ $SO_2$-S | **Model** $SO_4$-S/ $SO_2$-S |
|---|---|---|
| EMD | 0,084 | 0,049 |
| EMM | 0,004 | 0,081 |
| SS4 | 0,023 | 0,084 |

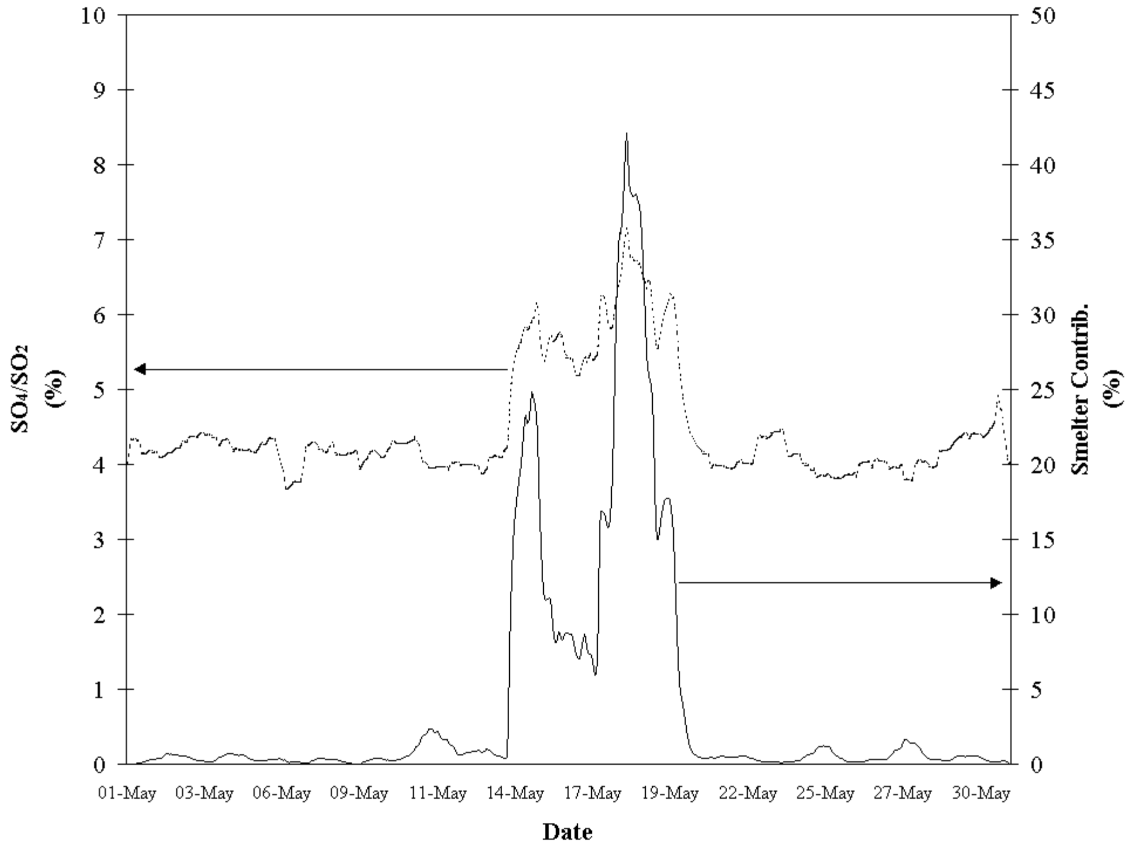


**Figure 3.10.** Twenty-four hours moving average of the $SO_2$-$SO_4$ ratio (%) and the contribution of the smelters to the total oxidized sulfur concentration (%) at Parque O'Higgins in downtown Santiago for May 1998.

*b) Santiago Area*

The model captures both the values and the horizontal gradients of the monthly average concentrations of $SO_2$ inside Santiago. Also, the variance of the concentrations is well simulated (See Table 3.7). However, significant discrepancies occur at La Florida (EML) and Las Condes (EMM) where the model underestimates the concentrations by a factor of up to five. This may be due to inaccuracies in the emission database for those areas and shortcomings in the representation of the local wind fields. We are in fact aware that the emissions of a significant $SO_2$ source, located in southwest of Santiago are strongly underestimated in the emission inventory (Fernández, pers. comm.). This could explain the systematic underestimate of the $SO_2$ concentrations at the southern stations (EML, EMQ and GMA). In an up-coming report we will use an up-dated emission inventory for which this bias has been corrected. In the case of Las Condes, the horizontal resolution precludes a satisfactory simulation of the meteorological fields. At Talagante, the bias is associated to too strong an advection of $SO_2$ emitted by sources in downtown

Santiago, especially in the first half of May when cloud cover is underestimated and the surface winds are consequently overestimated.

**Table 3.7**. Comparison between the model calculations and the observed monthly averages for the Santiago stations.

| | **EMB** | **EMD** | **EMF** | **EML** | **EMM** | **EMQ** | **GMA** | **SS4** |
|---|---|---|---|---|---|---|---|---|
| Observed Average | 29 | 28 | 30 | 29 | 13 | 20 | 28 | 2 |
| Standard Deviation | 26 | 27 | 25 | 34 | 10 | 28 | 25 | 2 |
| Model Average | 35 | 35 | 40 | 12 | 3 | 15 | 21 | 7 |
| Standard Deviation | 27 | 27 | 37 | 13 | 5 | 13 | 18 | 8 |
| Nº Obs. | 743 | 743 | 743 | 490 | 743 | 736 | 505 | 713 |

The daily averaged concentrations of $SO_2$ show maximal values between the $17^{th}$ and the $19^{th}$ at the downtown stations EMD and EMF (See Figure 3.11). Other high concentration episodes occur at the beginning and end of the month. Again, the underestimate of the $SO_2$ emissions in the southern part of the city becomes apparent in the model simulations. In fact, the simulated concentrations at EMQ and EML are noticeably lower than the observed concentrations (not shown here). Moreover, the simulations show a strong north-south gradient in $SO_2$ concentrations (See Table 3.7), which is not found in the measurements. The model captures the increase in $SO_2$ concentrations for the A type episode (May $15^{th}$-$19^{th}$). However, the model does not simulate the BPF type episode (May $8^{th}$). These two meteorological configurations, i.e., A and BPF, have different characteristics. The A type configuration is more defined and lasts longer than the BPF configuration (Rutllant and Garreaud, 1995). Apparently this makes the A type configuration easier to simulate than the BPF type configuration at least during the first half of May 1998 (Cf. Section 2).

The model correctly simulates the start of the A type episode on May $15^{th}$. However, while the observations show a sharp decrease in the $SO_2$ concentrations on May $19^{th}$ in connection with humid air advection from the coast, the model keeps high concentrations until May $22^{nd}$. Despite the model actually simulates some humidity advection associated with low level clouds on May $20^{th}$, it does not simulate the decrease in $SO_2$ concentrations. This is because the model has in its present configuration no representation of $SO_2$ transformation into sulfate due to low-level clouds or fog. The simulated concentrations of $SO_2$ do not fall until the synoptical conditions have completely changed. We illustrate this by showing the evolution of the boundary layer height (See Figure 3.12). According to the model, the stable conditions associated to the A type configuration remain from May $15^{th}$ until May $22^{nd}$. These results are consistent with an independent estimate of boundary layer height based on observed wind and temperature vertical profile at La Platina also shown in Figure 3.12 (Gomez, 2000). Notice that the agreement between the estimates of boundary layer height is better during the A type configuration than during the BPF configuration. During the A type configuration the radiative forcing dominates over the mechanical forcing of the vertical mixing. Moreover, during the first half of May the surface winds are overestimated by HIRLAM leading to too strong a vertical mixing in MATCH.

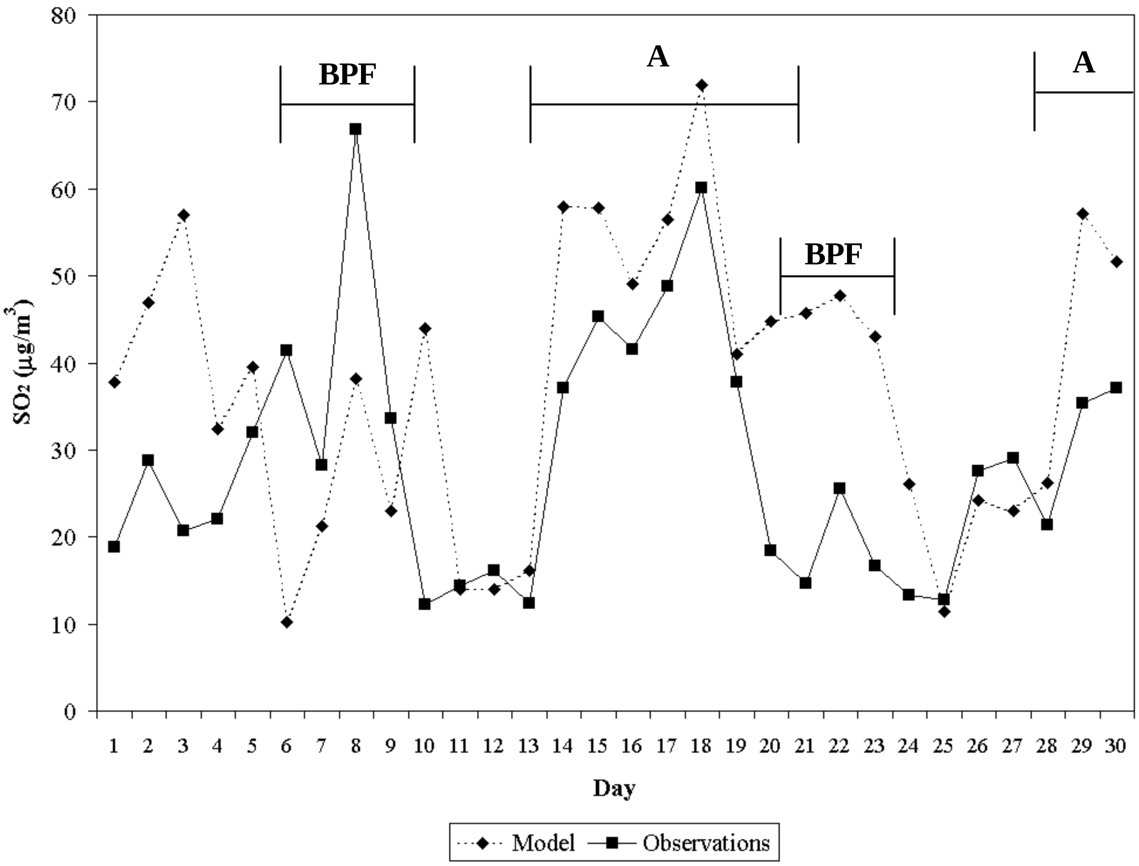


**Figure 3.11.** Daily averages for Santiago as calculated by the model and as observed, May 1998. $SO_2$ concentration in $\mu g/m^3$. The Santiago value was calculated as the average of the downtown stations (EMD and EMF).

The simulated diurnal variation of $SO_2$ concentrations is similar to the observed one at the Central Santiago stations (Parque O'Higgins, EMD and Av La Paz, EMF), i.e., a bimodal distribution, with maximal concentration in the morning and evening hours (See Figures 3.13). However, there is a mismatch in time and in magnitude, particularly for the evening maximum. The morning $SO_2$ maximum is simulated two hours earlier and the evening maximum is simulated five hours later than observed. This mismatch can be related to inaccuracies in the emission database used by the model, particularly the lack of a large sulfur source in southern Santiago. Such a point source could explain the early and broad afternoon maximum. Again, this will be discussed in more detail when applying an up-dated emission inventory for Santiago.

At the other Santiago stations, except at Las Condes, the model reproduces the general features of the observations. However, as indicated before, there is a significant systematic underestimate of the concentrations probably due to inaccuracies of the emission inventory in the southern part of the city. At Las Condes, the underestimate of the concentrations are probably due to the limited horizontal resolution used in the HIRLAM simulations (ca. 11 km) and the corresponding inability to simulate the details of the circulation near the Las Condes station.

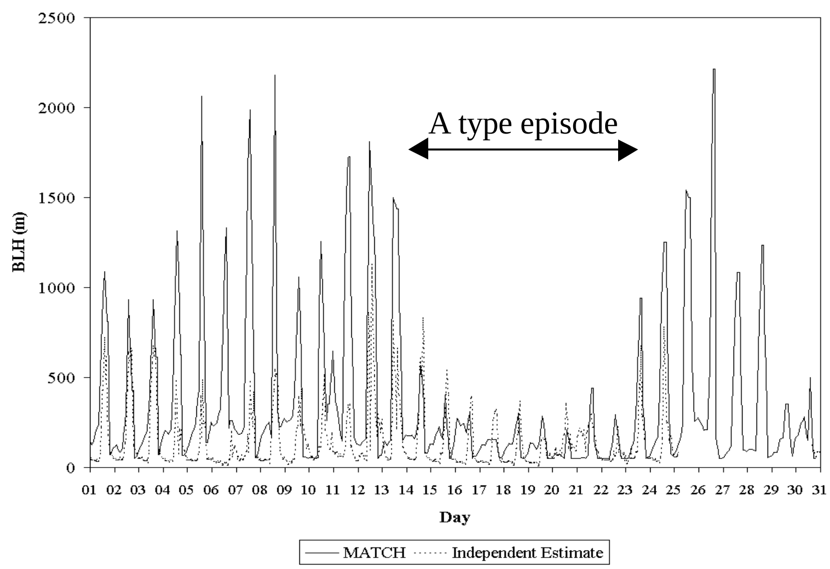


**Figure 3.12.** Boundary layer height (BLH) calculated by MATCH and from an independent estimate by Gomez (2000) for May 1998.

At Talagante, the model does not capture the diurnal variation of the $SO_2$ concentrations (See Figure 3.13 c). $SO_2$ shows a diurnal variation at Talagante with maximum concentrations in the early afternoon (ca. 2 p.m.). The model shows, on the contrary, highest concentrations during nighttime and early morning. We attribute this bias to too strong a radiative circulation as simulated by the meteorological model HIRLAM for the Santiago basin. This is particularly noticeable during the first ten days of simulations when HIRLAM underestimates the cloud cover (Cf. Section 2.5). This overestimate results in too strong an advection of $SO_2$-rich air from Santiago towards Talagante during nighttime. We illustrate these features by showing separately two periods: May 1$^{st}$ through May 13$^{th}$ and May 14$^{th}$ through May 23$^{rd}$ (See Figure 3.14). The former period coincides with the underestimate of cloud cover in HIRLAM and the corresponding overestimate of the nighttime advection of $SO_2$ emitted downtown Santiago in MATCH. The latter period corresponds to the A type configuration which is captured by HIRLAM and weak surface winds and advection prevail in the Santiago basin. When the advection from Santiago is overestimated in the first half of the month either the shape or the values of the concentrations are well simulated. In contrast, the model mimics the shape of the diurnal variation during the A type episode, however the contribution from the smelters seems to be overestimated. In the observations the maximum in $SO_2$ concentration coincides with the hours of maximum insolation. The model shows such a maximum too and it is associated to the strong vertical mixing that takes place at hours of maximum insolation which brings down $SO_2$-rich air from the upper model layers. However, the model indicates a nighttime maximum, which does not appear in the observations. The reasons for this nighttime maximum are not clear at the moment. However, we hypothesize that it could be related to shortcomings in the representation of the extreme static stability or to the lack of a $SO_2$-sink under foggy conditions, which may appear in nighttime in rural areas. On the other hand, as stated before, the very low values of $SO_2$ ($<2\ \mu g/m^3$) reported for nighttime at Talagante makes it difficult draw any definite conclusion at this stage.

a) EMD-EMF

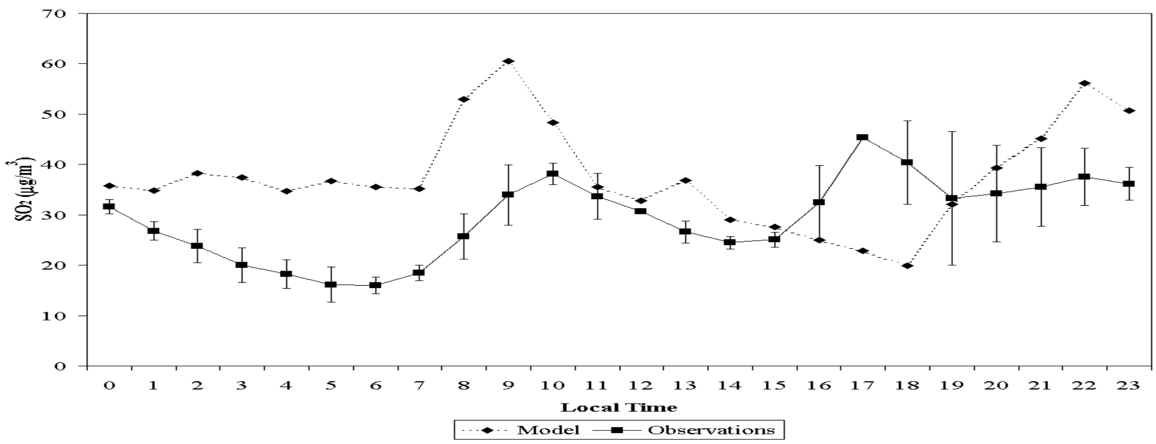


b) EMM

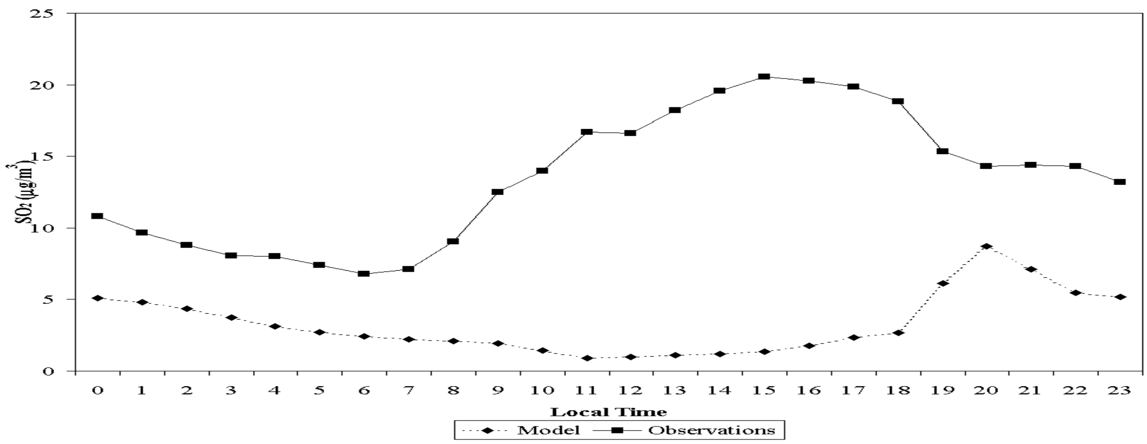


c) SS4

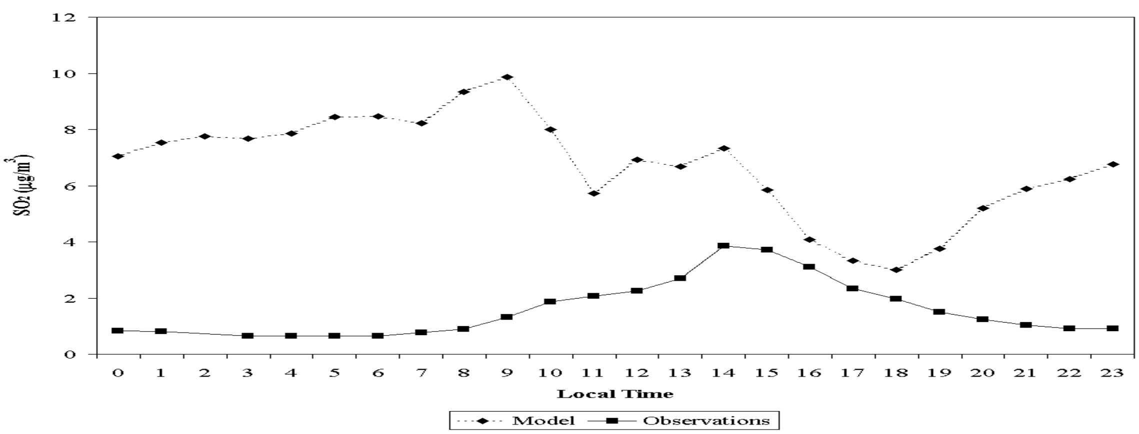


**Figure 3.13.** Diurnal variation for: a) Santiago (EMD and EMF); b) Las Condes; c) Talagante as calculated by the model and as observed for May 1998. $SO_2$ concentration in $\mu g/m^3$.

a) Talagante, first period, May 1st through May 13th.

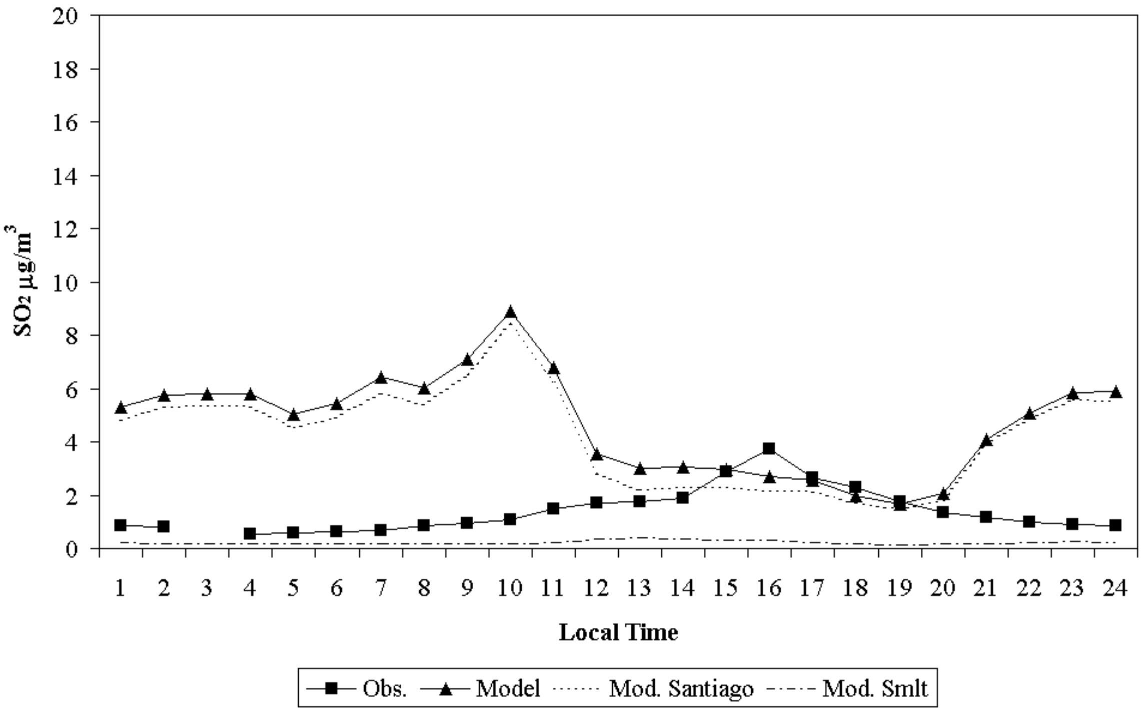


b) Talagante, second period, May 14th through May 23rd.

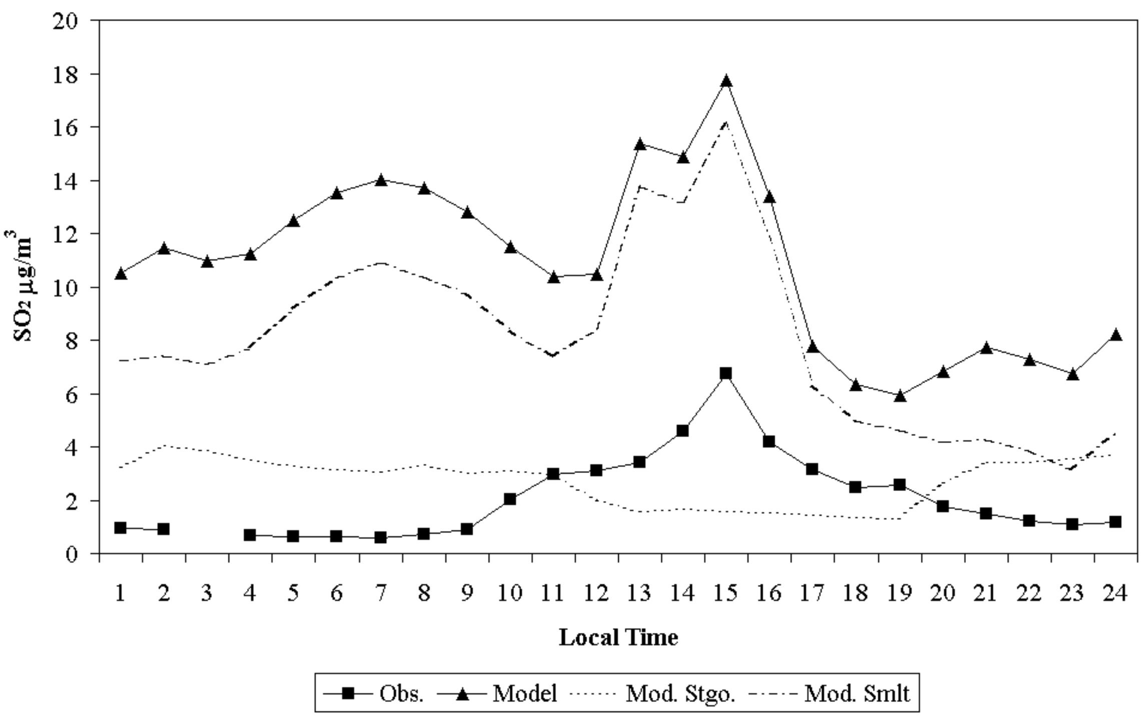


**Figure 3.14.** Diurnal variation at Talagante as calculated by the model and as observed for May 1998. The periods: May 1st through May 13th and May 14th through May 23rd are shown in separate panels. Also the contributions from the sources in Santiago and from the smelters are shown separately. $SO_2$ concentration in $\mu g/m^3$.

An objective comparison between the simulated and the observed $SO_2$ concentrations was made. The calculated statistics are presented in Table 3.8. Figure 3.15 shows a scatter plot of modeled and observed $SO_2$ daily averages for the Santiago stations. The model generally reproduces the $SO_2$ concentrations within a factor of two over Santiago. A better agreement, i.e., within a 25% is found in general at Parque O'Higgins (EMD). An exception to this occurs in connection with the first BPF situation in May $5^{th}$-$8^{th}$, when the model underestimates the cloud cover leading to too strong ventilation in Santiago. Another exception is related to the lack in the model of an $SO_2$ sink under foggy conditions. Thus, it seems that the EMD station in general captures the regional characteristics of the $SO_2$ dispersion.

**Table 3.8**. Statistics calculated from the $SO_2$ simulated and observed concentrations. See Appendix II for details.

| Statistics | Value |
|---|---|
| BIAS | 11 µg/m³ |
| RMS | 13 µg/m³ |
| Correlation | 0.5 |
| Nº Obs. | 283 |

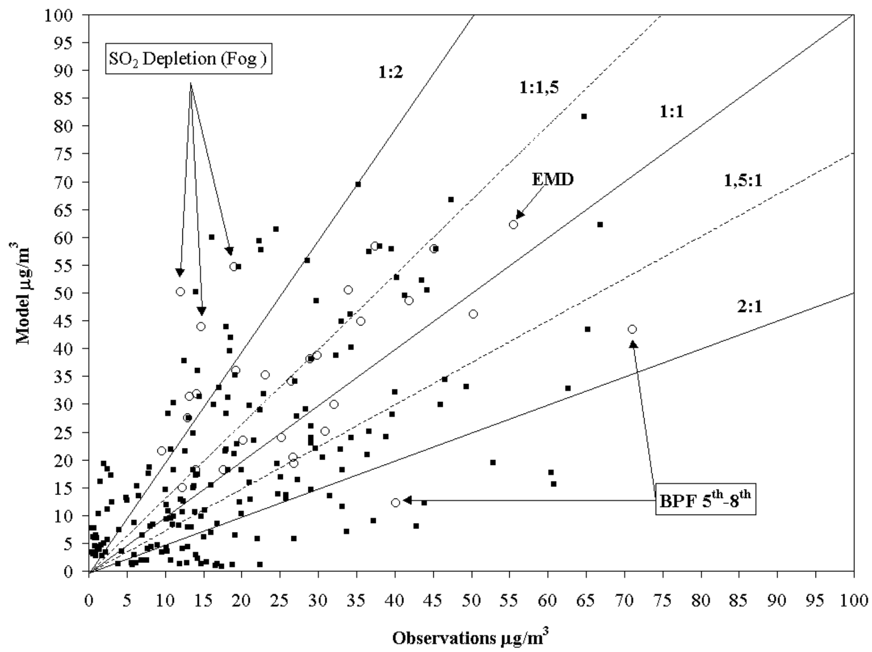


**Figure 3.15.** Scatter plot of the simulated and observed daily average $SO_2$ concentrations for the Santiago network. The circles indicate the values at the EMD station.

### c) $6^{th}$ *Region*

In the area where observations are available in the sixth region, the model simulates a strong diurnal cycle of the $SO_2$ concentrations due to the presence of a radiative circulation with up and down-slope winds along the Andes. According to the simulated wind circulation, $SO_2$-rich air is advected downwards from Caletones to the valley during nighttime resulting in high $SO_2$ concentrations. During daytime the contrary occurs leading to lower concentrations in daytime than in nighttime (See Figure 3.16). This is in fact observed at the Coya station (mCY) (See Figure 3.6). However, as addressed before, no such thing is observed at the other two stations available in the area, Coya Población (mCP) and Machalí (mML). Due to the limited resolution of the meteorological model the effects of the local circulations are not simulated at the mCP and mML stations (not shown here). The model does not "see" the east-west valleys where these stations are located and cannot simulate the possible layering effect discussed in Section 3.1.2.

Table 1.8 shows the comparison between the calculated and observed monthly averages at mCY, mCP and mML. The model roughly captures the gradient between the observed values at the Coya station and those observed down in the valley. However, the monthly averages $SO_2$ concentrations down in the valley (Machalí and Rancagua) tend to be slightly overestimated. This can be related to inaccuracies in the local emission inventory for Rancagua and to an overestimate of the downhill advection of $SO_2$ from Caletones during nighttime conditions. Again, it must be kept in mind that the model's present configuration (resolution) does not allow a detailed representation of the local wind circulations. We suspect that the actual circulations result in an inhibited impact from Caletones emissions down in the valley during nighttime.

**Table 3.9**. Comparison between the model calculations and the observed monthly averages at the 6th region stations. Notice that the model places mCY and mCP in the same grid-box. Unit: µg $SO_2/m^3$.

| | **mCY** | **mCP** | **mML** |
|---|---|---|---|
| Observed Average | 480 | 120 | 74 |
| Standard Deviation | 843 | 159 | 186 |
| Model Average | 700 | 700 | 170 |
| Standard Deviation | 930 | 930 | 290 |
| Nº Obs. | 743 | 743 | 743 |

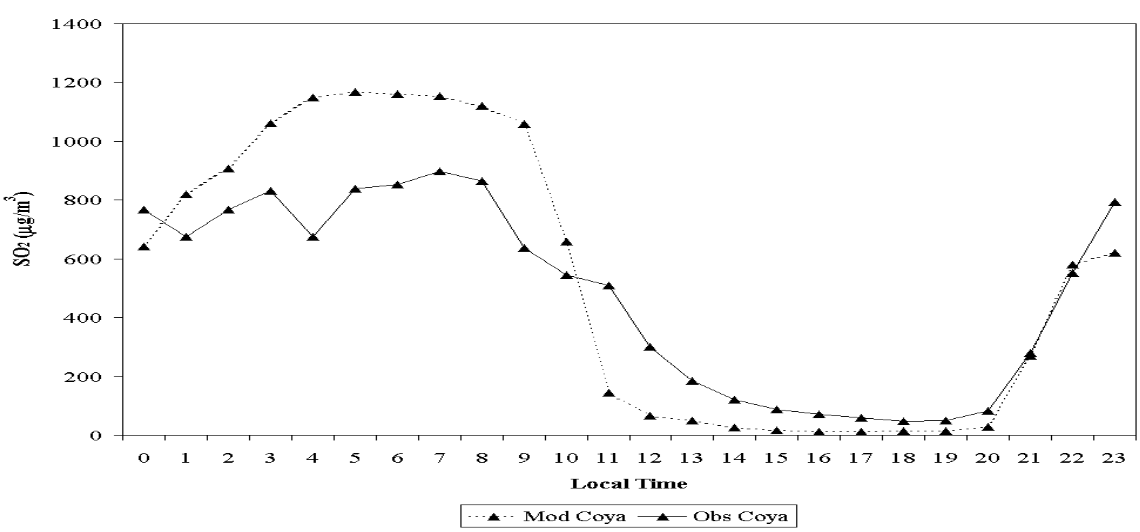


**Figure 3.17.** Observed and modeled diurnal variation for the Coya Club de Campo station in the 6th region, in May 1998. $SO_2$ concentration in µg/m$^3$.

On a daily average basis, one can see the changes in the concentrations due to the changes in the synoptical conditions. During May 1998, the most outstanding synoptical feature was the establishment of a strong low level low (A type episode) for a period of five days between May 15$^{th}$ and May 19$^{th}$. During that episode high concentrations of pollutants were observed in the boundary layer at all stations in Central Chile, also in the 6$^{th}$ region. The model reproduces in fact a rather strong stabilization in the boundary layer over the relatively flat areas during May 15$^{th}$ through May 19$^{th}$. However, in areas of steep topography, the effects of roughness counteract this stabilization. This limits the model's ability to reproduce the observed high concentrations during May 15$^{th}$ to May 19$^{th}$ at the sixth region stations. Nevertheless, under non-extreme conditions, the simulated daily average variation is roughly consistent with the observations.

*d) 5$^{th}$ Region*

The observation sites are located in five areas in the 5$^{th}$ region: around Ventanas copper smelter, near Chagres copper smelter, nearby Quillota where a number of power plants have been installed in the last few years and in the Viña del Mar and Valparaíso urban areas.

Near the coast, around the Ventanas smelter the model shows winds along a southwestern-northeastern axis. Theses winds advect the Ventanas plume to the northeast of the source during the day and to the southwest during the night. For all stations in the Ventanas network except Puchuncaví and La Greda, the model underestimates the monthly average of the $SO_2$ concentrations (See Table 3.10). We attribute this mismatch to an underestimate of the east-west wind component, which inhibits the impact of the Ventanas plume at these locations. The Puchuncaví station is located slightly northeast of the source where the simulated impact of the plume becomes more visible. The La Greda station is located very close to the smelter, in fact, the model places this station in the grid-box right to the north of the source, which explains the overestimate of the concentrations.

In the Valparaíso and Viña del Mar area, the model underestimates the concentrations. This is probably related to the fact that the relatively coarse resolution makes the model "blind" for the hills that surround Valparaíso and Viña del Mar allowing a too effective a ventilation of the area. However, an underestimate of the local emissions cannot be ruled out.

The model typically underestimates the monthly average of the $SO_2$ concentrations near the Chagres network stations. This can be partially explained because the model puts the Chagres emissions at 300 m and the stations are relatively close to the smelter. Thus the impact of the plume is underestimated at the surface near the source. Further, on the monthly average, the surface winds show a prevailing north-south direction, which inhibits the effect of the plume at the stations located along an east-west axis (See Figure 3.1).

For the Quillota network, a distinct diurnal cycle of $SO_2$ concentrations is observed (Cf. Section 3.1.2). The model does not reproduce this diurnal variation. Maximum concentrations are simulated during the night when stable meteorological conditions prevail. Minimum concentrations are simulated for the early afternoon when the vertical mixing is at maximum. We suspect that the mismatch between the simulations and the observations is due to the lack of a more detailed representation of the effects of the Aconcagua valley on the local winds. Particularly, the canyon effect that, in our opinion, may enhance the sea-breeze circulation. This is also reflected in the underestimate of the monthly average concentrations (See Table 3.10).

**Table 3.10**. Comparison between the model calculations and the observed monthly averages at the fifth region stations. Unit: $\mu gSO_2/m^3$.

| Station Code | Station | Model | | Observations | |
|---|---|---|---|---|---|
| | | Average | Maximum | Average | Maximum |
| mQT | Bomberos Quillota | 5 | 90 | 17 | 90 |
| CSP | Cajón San Pedro | 5 | 100 | 16 | 120 |
| UCV | Agro-UCV | 4 | 45 | 13 | 130 |
| mPV | Puchuncaví | 45 | 940 | 70 | 260 |
| MTN | Los Maitenes | 2 | 15 | 130 | 290 |
| GDA | La Greda | 480 | 2900 | 14 | 120 |
| VAG | Valle Alegre | 2 | 18 | 39 | 120 |
| SUR | Estación Sur | 134 | 1700 | 130 | 430 |
| MGT | Sta. Margarita | 7 | 200 | 59 | 160 |
| CMP | Lo Campo | 7 | 200 | 34 | 90 |
| mCM | Catemu | 0.5 | 5 | 28 | 70 |
| ROM | Romeral | 15 | 230 | 29 | 90 |

## 3.3. Conclusions

According to the model simulations, the regional distribution of oxidized sulfur is dominated by the contributions of the copper smelters, both horizontally and vertically. Only within the urban areas the contribution from local sources becomes significant (Cf. Figure 3.10).

When comparing the model simulations against available observations in Santiago, we find the best agreement at Parque O'Higgins and La Paz stations. This, in addition to the fact that these stations are located on a relatively flat area of the basin, not too close to large point sources, suggests that Parque O'Higgins is most representative of the regional patterns of dispersion of oxidized sulfur. Moreover, a similar behavior was found for the summer case (January 1998).

On a monthly average basis, the contribution from local sources in the urban area of Santiago shifts the partitioning of oxidized sulfur towards $SO_2$. However, there is an episodic impact of aged air masses with higher sulfate to $SO_2$ ratios. In fall, this impact appears to be related to the general subsidence conditions associated with low-level lows (A type configuration), whereas in summer it appears to be linked to vertical mixing at hours of highest insolation.

The emissions of a significant point source in southern Santiago are underestimated in the database. This leads to a systematic bias of the simulations for the southern and western part of Santiago. Other shortcomings in the simulations are due to too strong a thermally driven circulation as represented in HIRLAM for the Santiago basin in connection with underestimate of cloud cover, especially during the first half of May. For instance, at Talagante the impact of sources in downtown Santiago associated to the nocturnal wind circulation is clearly overestimated by the model during that period. Further, the model resolution in its present configuration is not enough to resolve small valleys making it unable to reproduce the observations at places like Las Condes.

Regarding the accuracy of the emission database, it must be pointed out that only preliminary inventories are available for urban areas other than Santiago. In addition, local emissions in the rural areas may be significant. Therefore, efforts should be made in order to provide better emission inventories for these areas.

The local character of the monitoring stations around the industrial complexes and within the urban areas limits a more detailed assessment of the performance of a regional model like HIRLAM-MATCH. Nevertheless, some regional features can be identified from the data collected at these networks. For instance the gradient in $SO_2$ concentrations over ten or more kilometers. The model generally captures this gradient for the Ventanas's and Caletones's monitoring networks as seen from the monthly averages. Other features in the observations appear to obey to local conditions in connection with particular topographical characteristics of the areas where the industrial complexes are located. These features are, of course, not well reproduced by the model. For instance, at Machalí neither the local emissions nor the local circulation driven by a complex topography are represented in the model, which makes the model unable to reproduce the diurnal cycle in $SO_2$ concentrations. Besides, at stations with strong local influences the comparisons between the model outputs and the observations may be misleading. Hence to perform a more complete evaluation of the performance of regional models like the HIRLAM-MATCH system, a regional monitoring network should be put in place. This is also important for assessing possible impacts on agriculture (García-Huidobro, 1999) and to define an appropriate base line for air quality. Particularly in view of the fact that urban areas and infrastructure in Central Chile, including interregional highways and trains, are expected to grow and develop further (PRDU, 1999).

## 4. SUMMARY AND PERSPECTIVES

Using the HIRLAM-MATCH modeling system, we have simulated the regional dispersion of oxidized sulfur in Central Chile for May 1998. This is an interesting period since an extreme pollution episode took place at that time. These simulations have been compared with the observations in order to assess the model performance under fall conditions. This exercise must be considered complementary to the summer case earlier presented (CONAMA-SMHI, 1999). Similarly as for the summer scenario, separate evaluations of the meteorological model (HIRLAM) and the dispersion model (MATCH) have been performed. Complementarily to this, an analysis of the $SO_2$ data provided by several networks for May 1998 has been performed.

Characteristics of the diurnal and the day-to-day (synoptical) variations were identified. Also, the partitioning between the $SO_2$ and sulfate reservoirs was preliminarily discussed. Distinct diurnal cycles in $SO_2$ were recognized at the majority of the monitoring stations. These cycles are typically associated with the presence of radiative circulations and variation in local emissions, mainly in connection with transportation sources. In addition to this, a strong day-to-day variation in the concentrations was identified. This variation is linked to the variations in the synoptical patterns that affected Central Chile in

May 1998. The most outstanding feature was a rather sever air pollution episode observed between May 15th and May 20th at all stations in Central Chile. This episode was associated with a strong low-level low (A type configuration), which gave stable meteorological conditions over all Central Chile. Less severe pollution episodes associated with stable conditions preceding a frontal passage (BPF type configuration) were also apparent from the observations, particularly in Santiago on May 8th.

Two month-long meteorological simulations using HIRLAM over Chile have been evaluated so far: January and May 1998. January 1998 was a summer period with little cloudiness in the Santiago area and thermally driven circulations with up and down-slope winds along the Andes. The simulation of January 1998 was very successful and judged to be accurate enough for dispersion modeling. The simulation for May 1998, which is a fall/winter month, is not as good as for January 1998. The fall/winter in the Santiago region is characterized by cloudy weather and low wind speeds. HIRLAM reproduces well the meteorological conditions associated with the onset of a coastal low in Central Chile moving southward along the coast (A type configuration). The prefrontal conditions ahead of a weak and often occluded front that slows down or becomes stationary (BPF type configuration) is less well captured. At least during the first half of May 1998. The disagreements are linked to underestimates of cloud cover, which in turn result in too strong radiative circulations. Nevertheless, the results presented here clearly indicate that HIRLAM is able to capture many of the meteorological features that are important for describing the dispersion of air pollutants over central Chile.

The predominance of the copper smelters as contributors to the burden of oxidized sulfur in Central Chile has been shown according to the MATCH simulations. As for the January 1998 scenario, the emissions from the copper smelters dominate the overall horizontal and the vertical distribution of sulfur in Central Chile. The urban emissions only affect significantly the city surroundings. The contribution of urban sources at rural sites as well as above the boundary layer is estimated to be less than a 10%. As in the summer case, the copper smelters contribute episodically to oxidized sulfur burden inside the urban areas, but apparently by different mechanisms in both seasons. During summer, the impact seems to be related to the strong vertical mixing that takes place during the afternoon. At this fall scenario, the impact appears to be related more to the strong general subsidence associated with the A type configuration than the afternoon vertical mixing. It must pointed out that the model shows a connection between the episodic impact of the copper smelters and the appearance in downtown Santiago of aged air masses with higher sulfate to $SO_2$ ratios, i.e., associated with secondary aerosols.

The majority of the available monitoring stations, both in Santiago and around industrial complexes in the 5th and 6th regions, have been placed to assess mainly local impacts, especially health effects. Therefore it cannot be expected that a regional model like HIRLAM-MATCH will be able to reproduce all the features of such observations. This is because either the local emissions are sufficiently specified or the meteorological fields are represented with enough precision. In other words, even though the model might accurately reproduce regional patterns of dispersion, it cannot be expected to reproduce the local patterns, associated for instance to a particular topographical feature (e.g., simulations at Machalí). In an up-coming report we will address some aspects relative to the design of a monitoring network to assess the regional distribution of pollutants.

Except for local effects, on a daily average basis the model generally reproduces the observations. Also the diurnal cycles are generally well simulated by the model.

However, significant discrepancies are found at some places. Some discrepancies occur are in connection with inaccuracies in the emission database (e.g. southwest Santiago). Some other are related to shortcomings in the representation of the meteorological field. At times, HIRLAM tends to overestimate the surface winds in connection with an overestimate of cloud cover. This results in the Santiago area in an overestimate of the $SO_2$ advection from downtown sources towards the surrounding areas (e.g., simulations for Talagante). This occurs especially during the first ten days of the HIRLAM simulations.

The model reproduces the concentrations observed during the A type episode (May $15^{th}$ – May $20^{th}$). However, the model does not capture the depletion of $SO_2$ associated with the advection of humid air (low-level clouds or stratus) from the coast. The model does in fact simulate advection of stratus from the coast at the end of the episode but it does not include a sink process in connection with foggy or high moisture conditions. Thus, work is left to be done in order to include explicitly transformation processes under such conditions. This will allow a better representation of the variations in the $SO_2$ concentrations under typical fall and winter situations.

The systematic evaluation of the model simulations allows us to identify shortcomings in the emission inventories (e.g., simulations for southwest Santiago). In this context, an accurate emission inventory outside Santiago turns out to be necessary to improve these simulations and any other dispersion modeling exercise in Central Chile. In addition to that, more regionally designed monitoring networks are necessary to ameliorate the evaluation of a modeling tool such HIRLAM-MATCH, especially outside the Santiago area.

The overall validation of the modeling tool will continue with an assessment of the model's ability to reproduce the meteorological and air quality observations for different seasons. In addition to the January and May 1998 scenarios already presented, a late spring and summer situation (November-December 1999), and two winter situations (May-June 1997 and June-July 1999) will be simulated. Also, in an up-coming report we will address the issue of the partitioning between the S-$SO_2$ and S-$SO_4$ reservoirs in more detail. The partitioning issue will be simultaneously addressed by applying HIRLAM-MATCH and the urban scale tool implemented in CONAMA-RM. With the aid of these tools we will interpret available measurements for winter 1999 that addressed secondary aerosols.

## 5. ACKNOWLEDGEMENTS

Discussions with Dr. René Garreaud and Dr. José Rutllant at the Department of Geophysics, University of Chile, have significantly improved the authors understanding of meteorological conditions in Chile and their help is gratefully acknowledged. Comments and discussions with CONAMA and SMHI staff are much appreciated too. This project is a part of the cooperation agreement between the Regional Government of Santiago in Chile and the County Administration of Västra Götaland in Sweden. This work is financed through the Chilean Commission for the Environment (CONAMA) and the Swedish International Development Cooperation Agency (SIDA).

## 6. REFERENCES

Artaxo, P., 1988. "Aerosol Characterization Study in Santiago de Chile Wintertime 1998". National Commission for the Environment, Metropolitan Region.

Cassmassi, J., 1999. "Improvement of the Knowledge of the Local Meteorology Conditions in the Metropolitan Region". Technical Report number 1. National Commission for the Environment, Metropolitan Region.

CENMA, 1998. "Proyecto Meteorología y Calidad del Aire". National Commission for the Environment, CONAMA.

CONAMA-RM, 1997: Plan de prevención y descontaminación atmosférica de la Región Metropolitana. Comisión Nacional del Medio Ambiente, Región Metropolitana de Santiago.

CONAMA-SMHI, 1999: Regional Dispersion of Oxidized Sulfur over Central Chile: A summer Case (Gallardo, L., Olivares, G., Aguayo, A., Langner, J, Aarhus, B. and Engardt, M.). Comisión Nacional del Medio Ambiente.

Cuxart, J., Bougealt, P., and Redelsperger, J. L. A turbulence scheme allowing for meso-scale and large-eddy simulations. *Q. J. R. Meteorol. Soc.* **126**, 1-30, 2000.

Flores, V., Gidhagen, L., et al. 2000. "Transporte Urbano y Medio Ambiente, Parte 4: Apoyo al Sistema de Información de la Calidad de Aire en Santiago". National Commission for the Environment, Metropolitan Region.

García-Huidobro, T., 1999. "A Risk Assessment of Potential Crop Losses Due to Air Pollution in the Central Regions of Chile". Imperial College of Science, Technology and Medicine. University of London, Centre for Environmental Technology.

Gómez, 2000. "Análisis de contaminantes atmosféricos en Santiago medidos por la red MACAM 2". Tesis para optar al título de Químico Ambiental. Departamento de Química, Facultad de Ciencias, Universidad de Chile.

IGM, 1988. "Atlas Geográfico de Chile para la Educación" Segunda edición, Instituto Geográfico Militar.

Jadrijevic et al, 1999: "Estudio de la calidad del aire en regiones urbano industriales de Chile". Informe final, fase intermedia. Comisión Nacional del Medio Ambiente, Departamento de

Koutrakis, P., 1999: Composition and sources of ambient particles in five Chilean cities: Iquique, Rancagua, Temuco, Valparaíso and Viña del Mar. Final Report . National Commission for the Environment.

Robertson, L., Langner, J., and Engardt, M. 1999: An eulerian limited-area atmospheric transport model. *J. Appl. Met.* 38, 190-210.

Rutllant, J. And Garreaud, R., 1995. "Meteorological Air Pollution Potential for Santiago, Chile: *Environmental Monitoring and Assessment*, 34, 223-244.

PRDU, 1999: Anteproyecto Plan Regional de Desarrollo Urbano y Territorial Región Metropolitana de Santiago, Memoria Explicativa. Intendencia Regional Metropolitana de Santiago, Secretaría Regional Ministerial de Vivienda y Urbanismo.

Sass, B. H., Nielsen, N. W., Jørgensen, J. U. and Amstrup, B. The operational HIRLAM system at DMI. Danish Meteorological Institute Technical Report 99-21, 1999. (Available from DMI (http://www.dmi.dk/f+u/)

Seinfeld, J and Pandis, S., 1998: Atmospheric Chemistry and Physics. From air pollution to climate change. J. Wiley and Sons, Inc.

# 7. APPENDIX I

**Table A1.** WMO-stations used in the evaluation. The three stations typeset in bold are also sounding stations. See also Figure 1.1.

| Station | Index number | Name | Latitude | Longitude | Elevation (m) |
|---|---|---|---|---|---|
| 1. | 85460 | Chañaral | -26.19 | -70.37 | 30 |
| 2. | 85470 | Copiapó | -27.18 | -70.25 | 290 |
| 3. | 85488 | La Serena | -29.54 | -71.12 | 142 |
| **4.** | **85543** | **Quintero Santiago** | **-32.47** | **-71.31** | **8** |
| 5. | 85574 | Pudahuel | -33.23 | -70.47 | 475 |
| 6. | 85577 | Santiago Q. Normal | -33.26 | -70.41 | 520 |
| 7. | 85586 | Santo Domingo | -33.39 | -71.37 | 75 |
| 8. | 85629 | Curico | -34.58 | -71.14 | 228 |
| 9. | 85672 | Chillan | -36.34 | -72.02 | 124 |
| 10. | 85682 | Concepcion | -36.46 | -73.03 | 12 |
| 11. | 85743 | Temuco | -38.45 | -72.38 | 114 |
| 12. | 85766 | Valdivia | -39.37 | -73.05 | 19 |
| 13. | 87121 | Tucuman Aero | -26.51 | -65.06 | 440 |
| 14. | 85486 | Vallenar | -28.36 | -70.46 | 526 |
| 15. | 87211 | Tingogasta | -28.04 | -67.34 | 1200 |
| 16. | 87213 | Chilecito Aero | -29.14 | -67.26 | 945 |
| 17. | 87217 | La Rioja Aero | -29.23 | -66.49 | 438 |
| 18. | 87305 | Jachal | -30.15 | -68.45 | 1175 |
| 19. | 87311 | San Juan Aero | -31.34 | -68.52 | 597 |
| 20. | 87320 | Chamical Aero | -30.22 | -66.17 | 467 |
| 21. | 87322 | Chepes | -31.20 | -66.36 | 658 |
| 22. | 87328 | Villa Dolores Aero | -31.57 | -65.08 | 561 |
| 23. | 87405 | Uspallata | -32.36 | -69.20 | 1890 |
| 24. | 87412 | San Carlos | -33.46 | -69.02 | 940 |
| 25. | 87416 | San Martin | -33.05 | -68.25 | 653 |
| **26.** | **87418** | **Mendoza Aero** | **-32.50** | **-68.47** | **705** |
| 27. | 87436 | San Luis Aero | -33.16 | -66.21 | 710 |
| 28. | 87448 | Villa Reynolds Aero | -33.44 | -65.23 | 485 |
| 29. | 87506 | Malargue Aero | -35.30 | -69.35 | 1426 |
| 30. | 87509 | San Rafael Aero | -34.35 | -68.24 | 745 |
| **31.** | **87715** | **Neuquen Aero** | **-38.57** | **-68.08** | **270** |
| 32. | 87129 | Santiago Del Estero Aero | -27.46 | -64.18 | 198 |
| 33. | 87222 | Catamarca Aero | -28.36 | -65.46 | 454 |
| 34. | 87244 | Villa De Maria Del Rio Seco | -29.54 | -63.41 | 341 |
| 35. | 87344 | Cordoba Aero | -31.19 | -64.13 | 484 |
| 36. | 87349 | Pilar Observatorio | -31.40 | -63.53 | 338 |
| 37. | 87453 | Rio Cuarto Aero | -33.07 | -64.14 | 420 |
| 38. | 87532 | General Pico Aero | -35.42 | -63.45 | 139 |
| 39. | 87623 | Santa Rosa Aero | -36.34 | -64.16 | 190 |
| 40. | 87736 | Rio Colorado | -39.01 | -64.05 | 79 |

**Table A2.** Stations in the Santiago area (see also Figure 1.2).

| Stations | Name | Latitude | Longitude | Elevation (m) |
|---|---|---|---|---|
| M01 | La Platina | -33.34 | -70.37 | 652 |
| M02 | Esc.Ingeniería | -33.27 | -70.39 | 534 |
| M03 | Los Tilos | -33.45 | -70.42 | 486 |
| M04 | Lo Pinto | -33.15 | -70.44 | 554 |
| M05 | Lo Cañas | -33.31 | -70.32 | 643 |
| M07 | Entel | -33.26 | -70.39 | 554 |
| M08 | Lo Prado | -33.27 | -70.56 | 1065 |
| M09 | San Cristóbal | -33.24 | -70.38 | 875 |
| M10 | Cuesta Chada | -33.55 | -70.39 | 696 |
| M11 | Codigua | -33.45 | -71.19 | 131 |
| M12 | María Pinto | -33.28 | -71.04 | 180 |
| M13 | Paine | -33.50 | -70.44 | 373 |
| M14 | La Campana | -33.38 | -70.57 | 483 |
| M15 | La Dormida | -33.03 | -70.59 | 1413 |
| M16 | Mallarauco | -33.34 | -71.09 | 156 |
| M18 | Cuesta Barriga | -33.33 | -70.56 | 883 |
| M19 | Quilapilún | -33.05 | -70.43 | 615 |
| M21 | Pirque | -33.39 | -70.36 | 676 |
| M22 | La Reina | -33.27 | -70.31 | 680 |
| M23 | El Manzano | -33.35 | -70.22 | 874 |
| M24 | El Paico | -33.42 | -71.00 | 255 |
| M25 | Polpaico | -33.09 | -70.52 | 520 |

# 8. APPENDIX II

Two indexes of error have been used: BIAS and RMS. These indexes are calculated as follows:

$$\text{BIAS} = \frac{\sum_{i=1}^{n_i}\sum_{j=1}^{n_j}(OBS_{ij} - MOD_{ij})}{n_i n_j}$$

$$\text{RMS} = \sqrt{\frac{\sum_{i=1}^{n_i}\sum_{j=1}^{n_j}(OBS_{ij} - MOD_{ij})^2}{\left(n_i n_j\right)^2}}$$

where $OBS_{ij}$ is the observed value and $MOD_{ij}$ is the simulated value on time i at the station j, for $n_i$ dates and $n_j$ stations.

The BIAS error indicates whether the model overestimates or underestimates the observed values. The RMS gives an idea of the absolute averaged difference between the simulated and the observed values.